A STUDY ON ACCELERATED CARBONATION CURING OF CONCRETE

BY

RIDA ALWI OTHMAN ASSAGGAF

A Thesis Presented to the
DEANSHIP OF GRADUATE STUDIES

KING FAHD UNIVERSITY OF PETROLEUM & MINERALS

DHAHRAN, SAUDI ARABIA

In Partial Fulfillment of the
Requirements for the Degree of

MASTER OF SCIENCE

In

CIVIL ENGINEERING

MAY 2016

KING FAHD UNIVERSITY OF PETROLEUM & MINERALS

DHAHRAN- 31261, SAUDI ARABIA

DEANSHIP OF GRADUATE STUDIES

This thesis, written by **RIDA ALWI ASSAGGAF** under the direction of his thesis advisor and approved by his thesis committee, has been presented and accepted by the Dean of Graduate Studies, in partial fulfillment of the requirements for the degree of **MASTER OF SCIENCE IN CIVIL ENGINEERING.**

Thesis committee

Prof. Shamshad Ahmad
(Advisor)

Dr. Salah U. Al-Dulaijan
Department Chairman

Prof. Mohammad Maslehuddin
(Member)

Prof. Salam A. Zummo
Dean of Graduate Studies

Prof. Omar S. Baghabra Al-Amoudi
(Member)

21/6/16
Date

This study is dedicated to my dear parents, my brothers, my sisters and my lovely wife

ACKNOWLEDGEMENT

In the Name of Allah the All-Merciful, the Ever Merciful. All perfect praise be to Allah, the Lord of the worlds, for guiding me and granting me patience, knowledge, courage, and health, to complete this research successfully. May the peace and blessings be upon our Prophet Muhammad, upon his household, his companions, and upon those following them in goodness until the Day of Judgment.

I would like to express my love and gratitude to my dear parents, my lovely wife, my brothers, my sisters and all my relatives for their love, encouragement and constant support, without them it would be difficult for me to achieve my educational goals.

Acknowledgement is also due to King Fahd University of Petroleum & Minerals and the Civil Engineering department for giving me the opportunity to complete my master degree and providing me the facilities that I need.

With boundless love and appreciation, I would like to express my heartfelt gratitude to the people who helped me bring this study into reality. I am very grateful to my advisor Prof. Shamshad Ahmad Saheb for his consistent guidance, ample time spent, and valuable advices that helped me bring this study into success. Working with him was an opportunity of great learning and experience. I am highly indebted and grateful to my committee members, Prof. Mohammad Maslehuddin Saheb and Prof. Omar S. Baghabra Al-Amoudi, for their technical support, suggestions and constructive comments during my research journey.

My special thanks goes to Eng. Saheed Kolawole Adekunle, for his support and help in scientific and experimental program, and to the concrete lab engineer, Engr. Syed Imran who spent a lot of his time helping me in the experimental program set up preparation. I owe all of you unreserved gratitude.

I am hugely indebted to Hadhramout Establishment for Human Development represented by Eng. Abdullah Ahmed Bugshan, for granting me a scholarship to help me during the whole period of my master degree.

Finally, thanks to all my friends in KFUPM, especially the Hadhrami community for creating the convenient atmosphere that helped us to overcome the immigration influence. May Allah continue to help and protect every one of you, Aameen.

Table of Contents

LIST OF TABLES

LIST OF FIGURES

LIST OF ABBREVIATIONS

°C	Degree Celsius
ACC	Accelerated Carbonation Curing
ANOVA	Analysis of Variance
ASTM	American Society for Testing and Materials
BASF	Badische Anilin und Soda Fabrik Company
df	Degrees of Freedom
DIN	Deutsches Institut für Normung
EDS	Energy-dispersive X-ray spectroscopy
FA	Fly Ash
GGBFS	Ground Granulated Blast Furnace Slag
GPa	Giga Pascal
KFUPM	King Fahd University of Petroleum and Minerals
LOI	Loss on Ignition
LSP	Limestone Powder
LVDT	Linear Variable Differential Transformer
MIP	Mercury Intrusion Porosimetry
MPa	Mega Pascal
MS	Mean Squares
NVC	Normally-Vibrated Concrete
OPC	Ordinary Portland Cement
RCPT	Rapid Chloride Penetration Test
RH	Relative Humidity
SCC	Self-Consolidating Concrete
SEM	Scanning Electron Microscopy
SF	Silica Fume
SIGAS	Saudi Industrial Gas Company
SP	Superplasticizer
SS	Sum of Squares
UHPC	Ultra-High-Performance Concrete
VMA	Viscosity Modifying Admixture
XRD	X-Ray Diffraction

THESIS ABSTRACT

Full Name	**ASSAGGAF, RIDA ALWI OTHMAN**
Title of Study	**A STUDY ON ACCELERATED CARBONATION CURING OF CONCRETE**
Major Field	**CIVIL ENGINEERING (STRUCTURES)**
Date of Degree	**MAY 2016**

Accelerated carbonation curing (ACC) is a new technique of concrete curing. It is a process involving forcing carbon dioxide gas to diffuse into a freshly prepared concrete under certain conditions, such as pressure, exposure duration, relative humidity, temperature, etc. Previous investigations in this field demonstrated that ACC improved the physico-mechanical properties and durability characteristics of concrete due to the resulting changes in the microstructure of concrete. In addition, ACC has economic and environmental benefits, such as serving as an avenue for consuming captured CO_2, thus helping to reduce the problems associated with CO_2 emission to the atmosphere.

The main goal of this research was to investigate the effect of ACC on the microstructure, physico-mechanical properties, and durability characteristics of concrete to decide whether it is possible or not to use ACC method in precast industries as a partial or full replacement of the conventional curing methods. This work was carried out in two phases: preliminary and detailed study. In the preliminary study, a concrete mixture was used to find out the optimum pressure and exposure duration for ACC. Based on the results of preliminary study, the optimal pressure and exposure duration for ACC were selected as 60 psi and 10 hours, respectively. Under the detailed study, a set of specimens of two mixtures of normally vibrated concrete (NVC), with and without mineral admixture, and two mixtures of self-compacting concrete (SCC) with mineral fillers were prepared and cured using ACC, under the optimum conditions obtained from the preliminary work. Another set of specimens were cured with burlap for 7 days as a control. The performance of ACC and burlap-cured concrete specimens was evaluated in terms of weight gain, carbonation depth,

mechanical properties and durability characteristics. SEM and XRD were also conducted on carbonated specimens to examine the effect of ACC on the concrete microstructure.

The increase in strength due to ACC for 10 hours was in the range of 34 to 79%, depending on the quantity of silica. Higher increase in strength due to carbonation was observed at lower silica from mineral admixture. The increase in strength after 7 days of air exposure followed by ACC was found to be in the range of 60 to 92%. The difference in strength of ACC and burlap-cured specimens was in the range of 5 to 26%. Tensile strength, modulus of elasticity, water penetration depth, and chloride permeability of ACC specimens were comparable with that of the burlap-cured specimens. Although, the shrinkage of ACC specimens was more than that of burlap-cured specimens, the 7th day shrinkage of ACC specimens was less or almost same as the permissible shrinkage, except for the SCC mixture with silica fume. SEM and XRD of the ACC specimens indicated the formation of calcite at the surface while the depth of carbonation did not exceed 2 mm for all the mixtures.

Based on the outcomes of this study, ACC method is recommended for curing precast concrete elements. Such curing while having no detrimental effect on the properties of concrete leads to CO_2 sequestration and reduction in green house gas emissions.

MASTER OF SCIENCE
KING FAHD UNIVERSITY OF PETROLEUM AND MINERALS
Dhahran, Saudi Arabia.

ملخص الرسالة

الاسم الكامل: رضا علوي عثمان السقاف

عنوان الرسالة : دراسة في تسريع معالجة الخرسانة بالكربونات

التخصص: هندسة مدنية (انشاءات)

تاريخ الحصول على الدرجة: مايو 2016 م

يعتبر تسريع معالجة الخرسانة بالكربونات (ACC) احد الطرق و التقنيات الحديثة للمعالجة. تعتمد فكرة هذه الطريقة على اجبار غاز ثاني أكسيد الكربون على اختراق الخرسانة حديثة العمر تحت ظروف معينة مثل الضغط، فترة التعرض، الرطوبة النسبية، درجة الحرارة، إلخ.

الأبحاث السابقة في هذا المجال أكدت أن هذه الطريقة (ACC) حسنت الخواص الفيزيائية والميكانيكية و دوامية الخرسانة كنتيجة للتغيرات التي تحصل في التركيب المجهري للخرسانة. بالإضافة الى ذلك، هذه الطريقة لها فوائد اقتصادية و فوائد بيئية كالحد من مشاكل انبعاث غاز ثاني أكسيد الكربون في الهواء.

الهدف الأساسي من هذا البحث كان دراسة تأثير هذه الطريقة على التركيب الداخلي للخرسانة والخواص الميكانيكية والفيزيائية وكذلك دوامية الخرسانة حتى يتسنى معرفة إمكانية استخدام هذه الطريقة في مصانع الخرسانة الجاهزة (مسبقة الصب) كبديل جزئي أو كلي للمعالجة بالطرق المستخدمة حاليا. الدراسة في هذا البحث نفذت على مرحلتين هما: الدراسة الأولية والدراسة التفصيلية. في مرحلة الدراسة الأولية لهذا البحث، تم استخدام عينات من الخرسانة لاكتشاف أفضل ضغط و أفضل فترة تعرض لغاز ثاني أكسيد الكربون. بناء على نتائج الدراسة الأولية وجد أن أفضل ضغط هو 60 باوند لكل إنش مربع و أفضل فترة تعرض لغاز ثاني أكسيد الكربون هي 10 ساعات. بعد ذلك و في مرحلة الدراسة التفصيلية، تم معالجة مجموعة من الخلطات الخرسانية العادية (NVC) و ذاتية الدمك (SCC)، والتي قد تحتوي في بعض الأحيان على إضافات كيميائية أو معدنية، بطريقة (ACC) و باستخدام أفضل ضغط وأفضل فترة تعرض واللذان تم الحصول عليهما في مرحلة الدراسة الأولية. أيضا تم معالجة مجموعة من العينات الخرسانية لنفس الخلطات و لكن عن طريق تغطيتها بالخيش (Burlap) المبلل بالماء لمدة 7 أيام و ذلك لمقارنة النتائج. لدراسة تأثير المعالجة المسرعة (ACC) على خواص الخرسانة، تم إخضاع العينات الخرسانية لعدد من الاختبارات و التي تشتمل على اختبار كمية استهلاك ثاني أكسيد الكربون، اختبارات الخواص الميكانيكية، اختبارات خواص دوامية الخرسانة و اختبار انكماش الخرسانة. و لدراسة التغيرات الداخلية للخرسانة تم أخذ صور مايكروسكوبية (SEM) للعينات بعد المعالجة و أيضا تم استخدام تقنية حيود الأشعة السينية (XRD) لدراسة التركيب الكيميائي و الخواص الفيزيائية و البلورية الحادثة بعد المعالجة.

لقد وجد أن الزيادة في قوة ضغط الخرسانة نتيجة استخدام طريقة (ACC) لمدة 10 ساعات فقط يتراوح بين 34 الى 79%، و ذلك يعتمد على كمية السليكا. لقد لوحظ أن هناك تناسب عكسي بين زيادة قوة ضغط الخرسانة و نسبة السيليكا الموجودة في الإضافات الخرسانية المستخدمة. أما الزيادة في قوة ضغط الخرسانة بعد معالجتها بـ (ACC) ثم تعريضها للهواء لمدة 7 أيام فقد وجد أنه يتراوح بين 60 الى 92%. على المدى البعيد، فرق القوة بين العينات المعالجة بـ (ACC) والعينات المعالجة بـ (Burlap) يتراوح بين 5 الى 26%. لقد وجد أن قوة الشد، معامل المرونة، مقاومة نفاذية الماء، مقاومة نفاذية الكلوريد في الخرسانة المعالجة بـ (ACC) مماثلة لتلك في الخرسانة المعالجة بـ (Burlap). على الرغم من أن درجة انكماش العينات المعالجة بـ (ACC) كانت أعلى في جميع الخلطات الخرسانية مقارنة بدرجة الانكماش للعينات المعالجة بـ (Burlap)، الا انها تقع ضمن الحد المسموح به للانكماش ما عدا عينات الخلطة الخرسانية ذاتية الدمك المضاف اليها غبار السيليكا. الصور المايكروسكوبية (SEM) للعينات بعد المعالجة و كذلك تقنية حيود الأشعة السينية (XRD) أثبتت تكون طبقة من الكربونات لا يتجاوز سمكها 2 مم في الخرسانة السطحية لجميع العينات المعالجة بـ (ACC).

بناء على نتائج هذا البحث، اتضح أنه بالإمكان استخدام طريقة (ACC) لمعالجة المنتجات الخرسانية في مصانع الخرسانة الجاهزة (مسبقة الصب). هذا النوع من المعالجة لا يصاحبه تأثير ضار على خواص الخرسانة بل على العكس من خلاله يمكن استهلاك ثاني أكسيد الكربون و الحد من الانبعاثات المسببة للاحتباس الحراري.

درجة الماجستير في العلوم
جامعة الملك فهد للبترول والمعادن
الظهران 31261
المملكة العربية السعودية

CHAPTER 1

INTRODUCTION

1.1 Introduction to accelerated carbonation curing (ACC)

Carbonation is the process in which the CO_2 gas present in the atmosphere penetrates into concrete and forms carbonic acid in the presence of moisture. The carbonic acid reacts with the $Ca(OH)_2$ of hydrated cement forming $CaCO_3$ [1]. The *long-term carbonation* in hardened concrete results in various changes in the microstructure of concrete. These changes include: (i) loss of alkalinity, which causes a decrease in the pH leading towards corrosion of steel bars embedded in concrete when pH falls below a threshold value of about 10, and (ii) decrease in the volume of hydration products, which causes contraction and leads to shrinkage in concrete, termed as carbonation shrinkage. Therefore, the long-term carbonation is considered harmful to the concrete durability characteristics.

Recently, some researchers explored the possibility of using the *short-term carbonation* (i.e., exposing concrete to CO_2 under pressure for a short duration) as an alternative method of curing concrete [2]. Such curing is termed as accelerated carbonation curing (ACC). In concrete subjected to ACC, an improvement was observed in the physico-mechanical properties and durability characteristics, such as increasing the density, strength, modulus of elasticity, sulfate resistance, and freeze-thaw resistance, and reducing the water absorption and chloride ions penetration [1], [3], [4]. Rostami et al. [11] reported that the reduction in pH mostly occurs at the surface concrete, and not in the core and, therefore, the reinforcement steel bars are safe from de-alkanization-induced corrosion.

The carbonation shrinkage resulting from ACC can be reduced by incorporating mineral admixtures, such as slag [3]. Zhan et al. [5] reported a lower drying shrinkage in the case of carbonation-cured concrete blocks than that measured on the same blocks, but moist-cured. The consumption of CO_2, captured from the manmade stationary sources of CO_2

emissions and stored for usage (carbon capture) in ACC of concrete would significantly reduce the global greenhouse gas emission and, therefore, the problems of global warming, which is of a great environmental concern globally. Monkman and Shao [6] have reported that the annual consumption of CO_2 in carbonation curing of precast concrete products in USA and Canada would be in the order of approximately 1.5 million tons, if recovered CO_2 is utilized and 1.0 million tons if the flue gas is utilized. According to another estimates, approximately 1.5 million tons of CO_2 can be sequestered in concrete products made with 16.4 million tons of cement, i.e., about 9% of CO_2 by mass of cement can be consumed in ACC of concrete products in USA [7].

Considering the technical and environmental benefits of ACC, this research was aimed at exploring the possibility of adopting the carbonation curing as a partial or full replacement of conventional curing methods for manufacturing of precast concrete elements [8].

1.2 Need for this research

Unlike the previous studies that used specific pressure and exposure duration, these two factors were varied in this research to find the optimum pressure and duration based on the maximum compressive strength gained. Furthermore, ACC was applied to four mixtures of concrete while most of the previous researchers used only paste or mortar.

The reported technical and environmental benefits, as discussed in the previous section, indicate that ACC can be adopted as an alternative curing method in precast concrete industries. The outcomes of the research would be utilized in reducing the curing time and effort in precast concrete production. This would help in improving the strength and durability of precast concrete products and make their production more environment-friendly, and probably faster than the conventional methods of curing.

1.3 Objectives

The main objective of the proposed work was to explore the possibility of using ACC as an alternative method of curing normally vibrated concrete (NVC) and self-consolidating concrete (SCC).

The specific objectives were as follows :

1. Select the optimum pressure and exposure duration for ACC.
2. Evaluate the performance of ACC in terms of the physico-mechanical properties, and durability characteristics of concrete.
3. Investigate the physico-chemical changes in the microstructure of concrete due to AC, and
4. Provide recommendations for ACC.

CHAPTER 2

LITERATURE REVIEW

The literature review presented in this chapter is meant to explain the mechanism and benefits of ACC, the factors affecting the effectiveness of ACC and the test methods adopted by previous researchers for evaluating the performance of concrete subjected to ACC.

2.1 Mechanism of ACC

The ACC of concrete is a process in which CO_2 sequestration is allowed to take place into concrete. Generally, the CO_2 sequestered into young concrete reacts with calcium compounds in cement, resulting into the formation of geologically stable calcium carbonates [1], [2], [4], [9]. The chemical reactions involved in the ACC process are as follows [10]:

$$3CaO \cdot SiO_2 + 3CO_2 + \mu H_2O \rightarrow SiO_2 \cdot \mu H_2O + 3CaCO_3 \quad (1)$$

$$2CaO \cdot SiO_2 + 2CO_2 + \mu H_2O \rightarrow SiO_2 \cdot \mu H_2O + 2CaCO_3 \quad (2)$$

$$Ca(OH)_2 + CO_2 + H_2O \rightarrow CaCO_3 + 2H_2O \quad (3)$$

The $CaCO_3$ formed due to carbonation reacts with calcium-silicate-hydrate (C-S-H) gel and provides a new gel structure better than the original C-S-H, resulting in improved mechanical properties and durability [1].

2.2 Benefits and advantages of ACC

Accelerated carbonation curing is found to change the mineralogy, morphology and microstructure of concrete, and it leads to an increase in the density of concrete, which implies better strength and durability than that offered by the microstructure of concrete developed by the conventional curing [1], [4], [9]. Although the ACC can lower the pH of

concrete by reducing the amount of $Ca(OH)_2$, the pH value of concrete is maintained well above reinforcement corrosion threshold value. Further, the acid and sulfate resistance of concrete can be increased due to the reduction in the amount of $Ca(OH)_2$. Therefore, ACC can be applied for curing of plain as well as reinforced precast concrete components [1], [11], [12]. Further, ACC reduces the curing time, compared with the conventional methods, and cost, compared with steam curing.

If the ACC is performed in a proper way, the technical and environmental benefits can be achieved as it helps in increasing the strength and durability characteristics of concrete, and in reducing the carbon footprint, a negative environmental concern associated with cement and concrete production.

2.3 Factors affecting the effectiveness of ACC

There are many factors reported in literature that affect the effectiveness of ACC [2]. The major factors can be classified into two categories, as follows:

1. *The exposure conditions for carrying out ACC*, such as the concentration of CO_2, temperature, relative humidity, pressure, and exposure duration in the carbonation chamber.

2. *Concrete composition and conditions before exposure to ACC*, such as age at demolding and exposure to CO_2, type and amount of binders, water/cement ratio, moisture content, and initial moist or steam curing.

Concentration of CO_2 to be maintained inside the ACC chamber was reported to be a highly influential factor. Researchers have tried several different CO_2 concentrations in the range of 14 to 25% for simulating the captured flue gas and also used 100% CO_2 concentration simulating the pure CO_2 recovered from flue gas [6], [10], [13], [14], [15]. Shao and Monkman (2006) have carried out the ACC using recovered CO_2 (100% concentration of CO_2) as well as flue gas having 25% concentration of CO_2 at a pressure of 5 bars (0.5 MPa) and curing duration of 2 hours and they reported the following results:

For 100 % CO_2 concentration

- CO_2 uptake was 16% by the mass of binder.
- Compressive strength of concrete was more than 60-days strength of conventionally cured concrete.

For 25 % CO_2 concentration

- CO_2 uptake was 9.7% by the mass of binder.
- Compressive strength of concrete cured using 25% CO_2 concentration was lower than concrete cured using 100% CO_2 concentration [10].

Different pressure values have been applied inside the curing chamber by previous researchers, varying between 1.45 and 72.5 psi. For more accuracy, some researchers vacuumed the chamber after placing the specimens inside and before injecting CO_2 gas. This process should be performed for a few seconds and under low pressure otherwise it will affect the porosity of concrete [3], [16], [17]. Moreover, researchers used different exposure durations to CO_2 gas. Shao [3] achieved CO_2 uptake in the range of 8 to 10% by the mass of binder and reported strength after 2 hours of carbonation curing equal to 80% of the strength after 24 hours of the conventional curing. Zhan et al. [16] conducted a study on ACC using recovered CO_2 (100% concentration of CO_2) maintaining a pressure of 1 bar (0.1 MPa), temperature in the range of about 26 to 30 °C and relative humidity in the range of about 82 to 95 % for a period of 6, 12 and 24 hours. They found an increase in the CO_2 uptake and strength, and a reduction in the drying shrinkage with increasing the duration of ACC.

ACC can be conducted directly after casting of concrete or after some initial air curing [17]. Rostami et al. [1] reported that keeping specimens in the air for a period before exposure to CO_2 gas is very important to allow better diffusion of CO_2 into concrete. The CO_2 uptakes were 8 and 23% for ACC done immediately after casting and ACC done after 18-hours air curing, respectively [17]. Kashef-Haghighi and Ghoshal [7], [18] have observed that the CO_2 uptake is adversely affected by the formation of layer of $CaCO_3$ during carbonation because the formed layer of $CaCO_3$ reduces the reactive surface area of

cement. Kashef-Haghighi and Ghoshal [7] found that the CO_2 uptake could be increased insignificantly in cases of cements having higher amount of reactive mineral and more fineness, which would provide a higher reactive surface area. Atiş [19] conducted a study on the ACC of concrete made by replacing normal Portland cement by 0, 50 and 70% of fly ash. He found no improvement in carbonation up to 50% replacement by fly ash. However, as compared to normal Portland cement, a higher carbonation was observed at 70% fly ash replacement. Shao and Monkman [3] have reported a positive impact of using slag as a partial replacement of cement. Their study, conducted on the evaluation of the performance of ACC of concrete made with cement partially replaced by 15, 25 and 50% slag, has revealed that the use of slag can be beneficial, as they noticed an increase in strength and resistance to de-icing salt, in addition to decrease in shrinkage. The positive effects of using reactive MgO as a partial replacement of normal Portland cement on the performance of accelerated carbonation-cured concrete have been reported by Mo and Panesar [20], [9].

Cement content and water/cement ratio are also reported to affect the effectiveness ACC. Jerga [21] has reported that the carbonation curing is more effective at a lower water/cement ratio and higher cement content. The effect of moisture content in concrete on carbonation curing is reported by Zou et al. [22], who have found that the degree of carbonation is higher when concrete has lower moisture content. The positive effect of initial steam curing before ACC is reported by Rostami et al. [11].

2.4 Test methods for evaluation of accelerated carbonation-cured concrete

The test methods used to evaluate the performance of concrete subjected to ACC, as reported by various researchers, are presented in the following subsections:

2.4.1 CO_2 uptake and degree of carbonation curing

The effectiveness of the ACC is either evaluated in terms of CO_2 uptake (by percentage of the mass of binder) or the CO_2 curing degree, defined as the ratio of the mass of CO_2 actually sequestered into concrete to the maximum theoretical mass of CO_2 possible to be sequestered by the binder [1], [11], [7], [16].

The expression for actual CO_2 uptake is given as [1], [11]:

$$CO_2 \text{ uptake } (\%) = \frac{(\text{Mass}_{\text{after carbonation}} + \text{Water}_{\text{lost}}) - \text{Mass}_{\text{befrore carbonation}}}{\text{Mass}_{\text{cement}}}$$

The expression for theoretical CO_2 uptake as given by Zhan et al. [16]:

$$CO_{2\%\ max} = 0.785(CaO - 0.7SO_3) + 1.091MgO + 1.42Na_2O + 0.935K_2O$$

Where, CaO, SO_3, MgO, Na_2O and K_2O are the oxide compositions of cement (% by mass of cement).

The expression for theoretical CO_2 uptake as given by Kashef-Haghighi and Ghoshal [7]:

$$CO_{2\%\ total} = 0.785(CaO - 0.56CaCO_3 - 0.7SO_3) + 1.091MgO + 1.42Na_2O + 0.935K_2O$$

2.4.2 Physico-Chemical Properties

Post-carbonation chemical composition and spatial distribution of hydration products, pH and microstructure of concrete are the principal physico-chemical properties, which are determined by most of the researchers to evaluate the performance of ACC. X-ray diffraction (XRD) analysis of the samples obtained by crushing slices taken at different depths from surface of carbonated concrete has been conducted for phase analysis to detect the presence of strong calcite peaks and a total absence of $Ca(OH)_2$ [1], [7], [9], [10], [11], [20], [23]. Scanning electron microscopy (SEM) image analysis, on concrete slices taken at different depths from surface of carbonated concrete, has been conducted for investigating the morphology of carbonates, i.e., spatial distribution of carbonate precipitates formed in the microstructure of concrete during ACC [1], [9], [20], [23]. To establish the carbonation front, pH test on the samples obtained by crushing slices taken at different depths from the surface of carbonated concrete has been conducted [9], [11], [23]. Mercury intrusion porosimetry (MIP) tests on the samples of carbonated concrete were conducted to determine the pore-size distribution [9], [23].

2.4.3 Physico-Mechanical Properties and Durability Characteristics

Tests to determine density, stress-strain behavior, compressive strength, modulus of rupture, modulus of elasticity, shrinkage, sorptivity, water permeability, chloride

permeability, sulfate and acid resistance have been conducted by researchers for evaluating the performance of ACC, in terms of improvements in the physico-mechanical and durability characteristics of carbonated concrete [9], [11], [21], [23], [24].

CHAPTER 3

METHODOLOGY OF RESEARCH

3.1 Introduction

In this chapter, the details of the materials used in the experimental work, preparation, casting and curing of test specimens are presented. Like the previous researchers who have attempted to study the effect of ACC on properties of concrete made using different mineral fillers [14], [25], in the present work, the ACC was used to cure concrete made with and without mineral admixtures. Two mixtures of normally vibrated concrete (NVC) and two mixtures of self-compacting concrete (SCC) studies are as follows:

M1: Plain Cement-NVC

M2: Cement and FA-NVC (FA: fly ash)

M3: SCC using LSP as Mineral Filler (LSP: limestone powder)

M4: SCC using LSP and SF as Mineral Fillers (LSP: limestone powder plus SF: silica fume)

The experimental program was conducted in two parts, preliminary work and detailed work.

3.2 Materials

3.2.1 Powders

- **Cement**

ASTM C 150 Type I cement (OPC) with a specific gravity of 3.15 was used in this study.

Table 3.1 shows the chemical composition of cement used in the present study.

Table 3.1: Chemical composition of Type I cement.

Component	Weight %
Oxide composition	
CaO	64.35
SiO_2	22.00
Al_2O_3	5.64
Fe_2O_3	3.80
K_2O	0.36
MgO	2.11
Na_2O	0.19
Equivalent alkalis	0.33
SO_3	2.10
LOI	0.70
Compound composition	
C_3S	55
C_2S	19
C_3A	10
C_4AF	7

- **Fly Ash (FA)**

Fly ash procured from the local market was used with the chemical composition given in Table 3.2.

Table 3.2: Chemical composition of fly ash (FA).

Component	Weight %
CaO	8.38
SiO_2	45.3
Al_2O_3	34.4
Fe_2O_3	2.37
K_2O	0.57
MgO	1.86
Na_2O	0.4
SO_3	0.46
LOI	3.5

- **Silica Fume (SF)**

Silica fume available in the local market was used with the chemical composition shown in Table 3.3.

Table 3.3: Chemical composition of silica fume (SF).

Component	Weight %
CaO	0.48
SiO_2	92.5
Al_2O_3	0.72
Fe_2O_3	0.96
K_2O	0.84
MgO	1.78
Na_2O	0.5
SO_3	---
LOI	1.55

- **Limestone Powder (LSP)**

The LSP used in this study was obtained from Abu Hadriyah quarry, Eastern Province of Saudi Arabia. This LSP has a specific gravity of 2.60 and its chemical composition is presented in Table 3.4.

Table 3.4: Chemical composition of limestone powder (LSP).

Component	Weight %
CaO	45.7
SiO_2	11.79
Al_2O_3	2.17
Fe_2O_3	0.68
K_2O	0.84
MgO	1.8
Na_2O	1.72
$Na_2O+(0.658K_2O)$	2.27
Moisture	0.2
LOI	35.1

3.2.2 Coarse Aggregates

Crushed limestone aggregates obtained from Abu Hadriah quarry were used in all concrete mixtures. The coarse aggregate had a maximum aggregate size of 12 mm, water absorption

of 1.4% and specific gravity of 2.60. The grading of the coarse aggregate is shown in Table 3.5.

Table 3.5: Coarse aggregate grading.

Sieve size (mm)	% passing			
	M1	M2	M3	M4
19	100	100	100	100
12.5	95	95	65	65
9.5	55	55	30	30
4.75	10	10	10	10
2.36	0	0	0	0

3.2.3 Fine Aggregates

Local dune sand with water absorption of 0.4% and specific gravity of 2.65 was used as the fine aggregate in all concrete mixtures. Grading of the dune sand is shown in Table 3.6.

Table 3.6: Fine aggregate grading.

ASTM Sieve #	Size	% passing
4	4.75 mm	100
8	2.36 mm	100
16	1.18 mm	100
30	600 µm	76
50	300 µm	10
100	150 µm	4

3.2.4 Chemical admixtures

- **Superplasticizer (SP)**

Glenium 51, a product of the Chemical Company BASF, was used as superplasticizer in this study. Table 3.7 shows the technical data pertaining to Glenium 51, as provided by BASF.

Table 3.7: Technical data of Glenium 51.

Appearance	Brown liquid
Specific gravity @ 20°C	1.08±0.02 g/cm^3
pH-value @ 20°C	7.0±1.0
Alkali content	≤ 5.0
Chloride content	≤ 0.1 %

- **Stabilizer/Viscosity Modifying Admixture (VMA)**

RheoMATRIX®100, a product of the Chemical Company BASF, was used as the stabilizer in SCC mixtures. It is available in the form of an aqueous solution of a high-molecular weight synthetic copolymer, which consists of a water-soluble polymer that is capable of modifying the rheological properties of a flowing concrete mixture. Table 3.8 shows the technical data of RheoMATRIX®100, as provided by BASF.

Table 3.8: Technical data of RheoMATRIX®100.

Appearance	Brown liquid
Specific gravity @ 20°C	1.0-1.02 g/cm^3
pH-value @ 20°C	6-9
Chloride content	≤ 0.1 %

3.2.5 Carbon Dioxide (CO_2) gas used for ACC

CO_2 with a high purity of 99.9% was utilized to cure concrete specimens. CO_2 gas was sourced from the Saudi Industrial Gas Company (SIGAS). Table 3.9 shows the details of the CO_2 analysis results, as provided by SIGAS.

Table 3.9: Analysis of CO_2 provided by SIGAS

Component	Limit	Act.
Assay	>=99.8%	99.9%
CO	<10 ppm	<10 ppm
NO	<2.5 ppm	<2.5 ppm
SO_2	<0.5 ppm	<0.5 ppm
NO_2	<2.5 ppm	<2.5 ppm
Water	<32 ppm	<32 ppm
H_2S	<0.5 ppm	<0.5 ppm

3.2.6 Mixing water

A normal sweet water was used for mixing and conventional curing of concrete specimens.

3.3 ACC set up

A purpose-built ACC cylindrical chamber was fabricated, as shown in Figure 3.1. The cylindrical shape was chosen to sustain more pressure. The inside diameter and height of the chamber were 40 and 50 cm, respectively. To place the concrete specimens inside the chamber, a 25 cm diameter hole was made at the top of the chamber with 35 cm cover plate. For ensuring the safety, the chamber was made of steel with a wall thickness of 8 mm. Two holes, one as inlet and another as outlet, were made through the wall. The inlet was connected to the CO_2 cylinder by a pipe and the outlet was connected to a pressure gauge to measure inside chamber pressure. To prevent corrosion of the steel wall, the wall was epoxy-coated. The schematic diagram of the set-up is shown in Figure 3.2.

Figure 3.1: Set-up for the ACC.

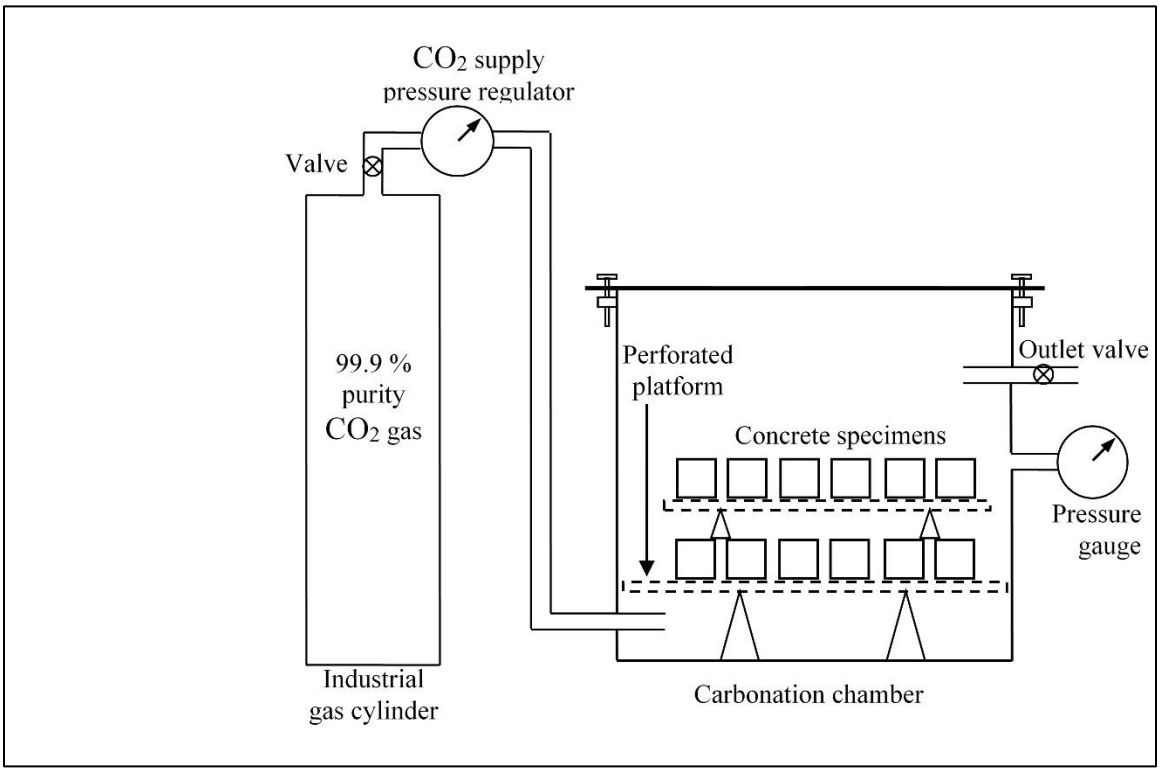

Figure 3.2: Schematic diagram of ACC set-up

3.4 Details of Concrete Mixtures

Table 3.10 shows the details of the four concrete mixtures used in this study.

Table 3.10: Details of the concrete mixtures.

Weight of one cubic meter of concrete				
Concrete Mixture →	**M1**	**M2**	**M3**	**M4**
w/p ratio	0.45	0.45	0.3	0.3
Fine/Coarse aggregate ratio	0.667	0.667	1	1
Fine/Total aggregate ratio	0.4	0.4	0.5	0.5
W (kg)	194	194	165	165
SP (g)	0	0	10000	9000
VMA (g)	0	0	6250	7500
C (kg)	375	300	400	400
FA (kg)	0	75	0	0
SF (kg)	0	0	0	50
LSP (kg)	0	0	100	50
Total cementitious material (kg)	375	375	500	500
12.5 mm (kg)	53.7	53.7	293	292
9.5 mm (kg)	429.8	429.8	293	292
4.75 mm (kg)	483.5	483.5	167	167
2.36 mm (kg)	107.4	107.4	84	83
Total coarse aggregate (kg)	1074.4	1074.4	837	834
Fine aggregate (kg)	716	716	837	833
Total aggregate (kg)	1790.4	1790.4	1674	1667

3.5 Preparation of mixtures

The following procedure was used for preparation of concrete mixtures M1 and M2:

- Concrete dry components, such as cement, fly ash, aggregate, etc., were weighed accurately.
- Before starting mixing, inner surface of the mixer was wetted with water to avoid loss of some of mixing water.

- After placing the ingredients in the mixer, dry mixing was started and continued for approximately one minute. The drum opening was covered with a lid to keep powder dust inside.
- Half of the water was added during mixing until aggregate and sand were coated with wet cementitious materials. Then, the drum cover was removed. This process lasted for one to two minutes.
- Another half of the water was added gradually and then the drum was kept rotating for about three minutes until the mixture was homogenous. Figure 3.3 shows the mixer used.

Figure 3.3: Laboratory electric mixer.

For SCC mixtures M3 and M4, the same method of preparation, as summarized above, was used except that the SP and VMA were added and mixed with the second half of water and also the mixing time from adding the second half of water until finish was longer, approximately 15 to 20 minutes.

3.6 Preliminary Work

This part of study was conducted to obtain the optimum exposure duration and pressure for carrying out ACC effectively. For this purpose, concrete specimens were prepared using mixture M1 and after 18 hours of casting, these specimens were demoulded and subjected

to ACC curing for different sets of ACC durations and pressures. Based on maximum gain in compressive strength, an optimum set of duration and pressure for ACC was selected. This part also included to determine the post-ACC optimum duration of air curing. After finalizing the optimum duration and pressure for ACC, the specimens that were cured using ACC were kept under air curing for different durations for selecting the optimum duration of post-ACC air curing based on development of maximum strength.

3.6.1 Standardization of the reference concrete mixture

Since the preparation of concrete specimens for ACC was done in batches, the reference mixture (i.e., mixture M1) was standardized. It was required to ensure that the measured strength of the carbonation-cured concrete specimens at various pressures and durations would be compared to approximately the same initial strength of concrete before ACC. In other words, the standardization process aimed at making sure that each batch of concrete mixture has the same initial compressive strength, within a narrow range of deviation. The gross material properties of a highly heterogeneous material like concrete are significantly affected by variations in a host of mixing and ingredient parameters, even if the mixture proportions do not change. This idea of mixture initial strength standardization will eliminate the effect of significant differences in the initial strengths, which may be difficult to account for, from the overall response of the carbonation-cured concrete specimens. Consequently, the measured responses can be attributed only to variations in the two experimental parameters: carbonation pressures and exposure duration.

For the initial strength standardization of the reference concrete mixture M1, specimens were prepared in three batches, each batch with the same mixture proportions, aggregate type and gradation, and mixing procedure. Immediately, after completion of mixing, the slump was measured and the mixture was cast in 50 mm cube molds. The exposed concrete top surfaces in molds were protected from evaporation with the aid of plastic sheets. After 18 hours of post-casting curing in the mold in the laboratory condition at 23±2 °C, the concrete specimens were demolded and tested immediately for initial compressive strength at a loading rate of 1 kN/s, corresponding to 0.4 MPa/s. Each of the three batches of concrete contained twelve 50 mm cube specimens. The compressive strength test results

of the specimens belonging to three batches were analyzed for adopting the mixing procedure for standardization of the initial strength.

Figure 3.4 shows the normal probability density distributions for the three batches of the mixture. As can be seen from Figure 3.4, batch 3 exhibited the least spread of compressive strengths. Table 3.11 shows the statistics of the compressive strength test results of the three batches of concrete M1 mixture used for standardization of reference concrete mixture. It is clear from Figure 3.4 and Table 3.11 that the batch 3 had lowest spread of strengths, as indicated through various statistical parameters, such as standard deviation and coefficient of variance (COV). Therefore, for all the concrete batches used in the preliminary study, the mixing procedure of batch 3 was adopted. This criterion of acceptance of the batches qualified for ACC, based on a standardized initial strength of M1 mixture in the range of 16.0 ± 2.0 MPa, was adopted.

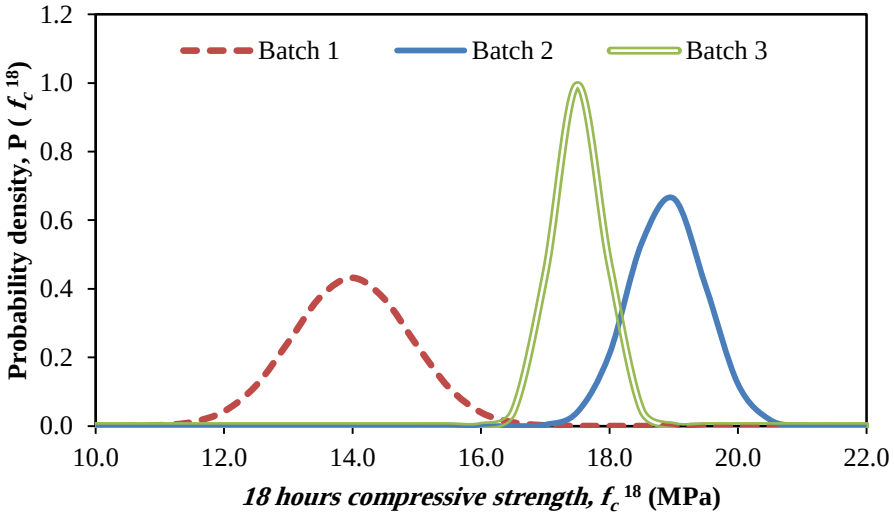

Figure 3.4: Distribution of compressive strengths of batches standardization of reference concrete mixture.

Table 3.11: Compressive strength (MPa) statistics of batches standardization of reference concrete mixture.

	Batch 1	Batch 2	Batch 3
No. of specimens	12	12	12
Minimum	12.4	17.9	16.8
Maximum	15.1	20.2	18.0
Range	2.6	2.4	1.2
Average	14.0	18.9	17.5
Standard dev.	0.92	0.59	0.40
COV	6.6%	3.1%	2.3%

3.6.2 Optimization of pressure and CO_2 exposure duration for ACC

The CO_2 intake and penetration through concrete mainly depends on the pressure intensity, exposure duration and concrete age at curing time. Table 3.12 presents some useful information pertaining to these factors, as reported in literature.

In this study, concrete specimens were left for 18 hours in the molds while covering the top surface for preventing the evaporation of water from the specimens. After 18 hours, the specimens were demoulded and placed inside the ACC chamber. No vacuum pump was used to suck air before carbonation. Instead, the outlet was left open for one minute to flush out the normal air from the chamber.

Following are the details of specimens and combinations of CO_2 pressures and exposure duration to determine the optimum conditions of ACC:

- Total six batches of normal concrete specimens were cast using mixture M1. Each batch had 44 cubes of 50 mm size. After casting, the specimens were subjected to initial air curing for 18 hours in an environment of 60% RH and 25°C, then demolded and cured by ACC.
- To get the initial strength for each batch, the first four cubes were crushed directly after demolding without ACC.
- Different combinations of six pressures (10, 20, 30... and 60 psi) and ten exposure durations (1, 2, 3… and 10 hours) were chosen to carry out ACC for finding the optimum combination of pressure and exposure duration to be used for ACC

throughout the present study. Four cubes were used for each combination of pressure and CO_2 exposure duration. A pure CO_2 gas was used (99.9% CO_2 concentration). After taking out the specimens from the ACC chamber and leaving for 1 hour in air, they were crushed by applying load at a rate of 1 kN/s to obtain average compressive strength.

- The weight gained after carbonation was recorded using a high-sensitivity (0.01g precision) electronic balance.
- Figure 3.5 shows samples preparation and compression testing machine.

The procedure of curing is as follows:

- The CO_2 gas supply was opened, while the chamber outlet valve remained opened for about 1 minute, and then the outlet valve was closed. This process was intended to flush out the air from the chamber, so that the chamber will be almost fully filled by CO_2 gas.
- The gas flow rate was regulated and stabilized over about 2 minutes, using the pressure gauge mounted on the chamber. This was done to maintain a constant intended pressure for ACC.
- After 1 hour of exposure to the set pressure, the gas supply was closed, and the chamber was depressurized in order to retrieve the 1-hour CO_2 cured batch. With the cube specimens for longer durations still left in the chamber, the chamber was closed, and the steps 1 through 3 above was repeated for other longer curing durations.

The final outcomes of this part of the study indicates that the optimum pressure and ACC duration to be **60 psi** and **10 hours**, respectively, since the compressive strength and weight gained after carbonation were the highest and the CO_2 gas did not penetrate the specimens to the core. Detailed test results and discussion regarding the selection of optimum pressure and duration for ACC is presented in Section 5.1.

Table 3.12: Previous research data of used pressures and durations.

Reference	Period before demolded and exposure to CO_2	Evacuation pressure (psi)*	Maintained pressure inside the chamber (psi)*	Exposure duration
Shao, Y., et al., (2014) "Accelerated Carbonation of Portland Limestone Cement."	18 hours	--	21.75	2 hours
Zhan, B., C. Poon, et al. (2013). "CO_2 curing for improving the properties of concrete blocks containing recycled aggregates."	Immediately demolded and placed in the chamber	7.25	1.45	6,12 and 24 hours
Mo, L. and D. K. Panesar (2013). "Accelerated carbonation – A potential approach to sequester CO_2 in cement paste containing slag and reactive MgO."	24 hours	--	14.7	7, 28, and 56 days
El-Hassan, H., Y. Shao, et al. (2013). "Reaction Products in Carbonation-Cured Lightweight Concrete.pdf."	18 hours	10.15	14.5	4 hours
Rostami, V., Y. Shao, et al. (2012). "Microstructure of cement paste subject to early carbonation curing."	18 hours	--	21.75	2 hours
Mo, L. and D. K. Panesar (2012). "Effects of accelerated carbonation on the microstructure of Portland cement pastes containing reactive MgO."	24 hours	--	14.7	7, 28, and 56 days
Rostami, V., Y. Shao, et al. (2011). "Durability of concrete pipes subjected to combined steam and carbonation curing."	18 hours	--	21.75	2 hours
Monkman, S. and Y. Shao (2010). "Carbonation Curing of Slag-Cement Concrete for Binding CO_2 and Improving Performance."	Immediately demolded and placed in the chamber	7.25	21.75	2 hours
Shao, Y., X. Zhou, et al. (2006). "A New CO_2 Sequestration Process via Concrete Products Production."	Immediately demolded and placed in the chamber	7.25	72.5	2 hours
Monkman, S. and Y. Shao (2006). "Assessing the Carbonation Behavior of Cementitious Materials."	Immediately demolded and placed in the chamber	7.25	72.5	2 hours

* 1 MPa = 145 psi

Figure 3.5: Preparation of preliminary work specimens.

3.6.3 Optimum duration of air curing after optimal ACC

Optimum ACC and 7-days burlap curing were conducted on four selected concrete mixtures. Thereafter, the specimens were exposed to air and tested for compressive strength at different ages. This was done to select an optimum duration of air curing of concrete in post ACC and post burlap curing scenarios based on the effective gain of compressive strength. The procedure used for this purpose is summarized below:

- Four different concrete mixtures that were considered are as follows: Plain Cement-NVC, Cement and FA-NVC, SCC using LSP as Mineral Filler, SCC using LSP and SF as Mineral Fillers.
- For each mixture, cubical specimens of 50 mm size were cast. A set of four cubes were tested for compressive strength immediately after demolding to determine the initial strength.

- After demoulding and initial strength testing, the specimens were divided in two groups. One group of specimens was subjected to optimum ACC and another group was cured using burlap. After ACC and burlap curing, the specimens were exposed to air.
- Compressive strength tests were conducted after 7, 14, 28 and 90 days of air curing.
- Based on the analysis of detailed test results, as presented in Section 5.4, the optimum duration of air curing after optimum ACC was found to be **7 days** for all the mixtures.

3.7 Detailed Work

The selected optimum pressure and duration of ACC through the preliminary work, as described in previous section, were used to cure the four different types of concrete mixtures. The effects of optimal ACC and air curing on the performance of the concrete mixtures were evaluated in terms of their physico-chemical properties, CO_2 intake, carbonated depth, mechanical properties, shrinkage, and durability characteristics, as detailed in the subsequent chapters.

CHAPTER 4

EXPERIMENTAL WORK

4.1 Introduction

This chapter presents details of preparation and testing of concrete specimens belonging to four different mixtures to investigate the effects of *optimal ACC* and air curing on their physico-chemical properties, CO_2 intake, carbonated depth, mechanical properties, shrinkage, and durability characteristics. The mechanical tests included compressive and splitting tensile strength tests and static modulus of elasticity test. Water permeability, chloride permeability and electrical resistivity tests were conducted to determine the durability characteristics. The tests used for physico-chemical properties were SEM and XRD.

4.2 Casting and curing of specimens

For each mixture, the specimens required to conduct various tests were cast. That included specimens of various sizes and different shapes (cubical, cylindrical, prism, etc). For SCC mixtures (M3 and M4), there was no vibration used for compaction. Conversely, the vibration was applied for NVC mixtures (M1 and M2). Three replicate specimens were used to obtain average test results as representative values. Figure 4.1 shows the specimens prepared for conducting different tests for one of the four concrete mixtures. As shown in Figure 4.1, mixture ID, test type, specimen number and curing regime were written on each sample.

Half of the specimens were then placed inside ACC chamber after recording the initial weight for each specimen. The other half were covered with wetted burlap for one week. After both types of curing, all the specimens were exposed to air in laboratory at normal room temperature of 25°C until the date of testing.

Figure 4.1: Specimens prepared for different tests.

4.3 Details of the specimens for different tests

Table 4.1 shows the details of concrete specimens used for conducting various tests for each of the selected four mixtures of NVC and SCC.

4.4 Weight gain

The weight, before and after ACC, was recorded for all concrete specimens. A sensitive electronic balance was used to get accurate values. Figure 4.2 illustrates the weighing process for one sample before and after ACC. The net weight was then obtained. The weight gains were expressed in terms of percentages of the cement mass.

Table 4.1: Details of specimens required for various tests per mixture

S/N	Test	Test Method	Specimen Dimensions	Test Age
1	Weight gain	Mass gain	For all specimens	Before and after carbonation
2	Carbonation depth	Phenolphthalein spray	50 x 50 x 50 mm cube	Immediately after ACC
3	Compressive strength	ASTM C 39	50 x 50 x 50 mm cube	7, 14, 28 and 90 days
4	Tensile strength	ASTM C 496	75 x 150 mm cylinder	14 days
5	Modulus of elasticity	ASTM C 469	75 x 150 mm cylinder	14 days
6	Water permeability	DIN 1048	100 mm cube	14 days
7	Chloride permeability	ASTM C 1202	75 x 150 mm cylinder	14 days
8	Shrinkage	ASTM C 157	50 x 50 x 250 mm prism	Up to 6 months
9	Morphology of the microstructure	SEM	50 x 50 x 50 mm cube	Immediately after ACC
10	Mineralogy of the microstructure	XRD	50 x 50 x 50 mm cube	Immediately after ACC

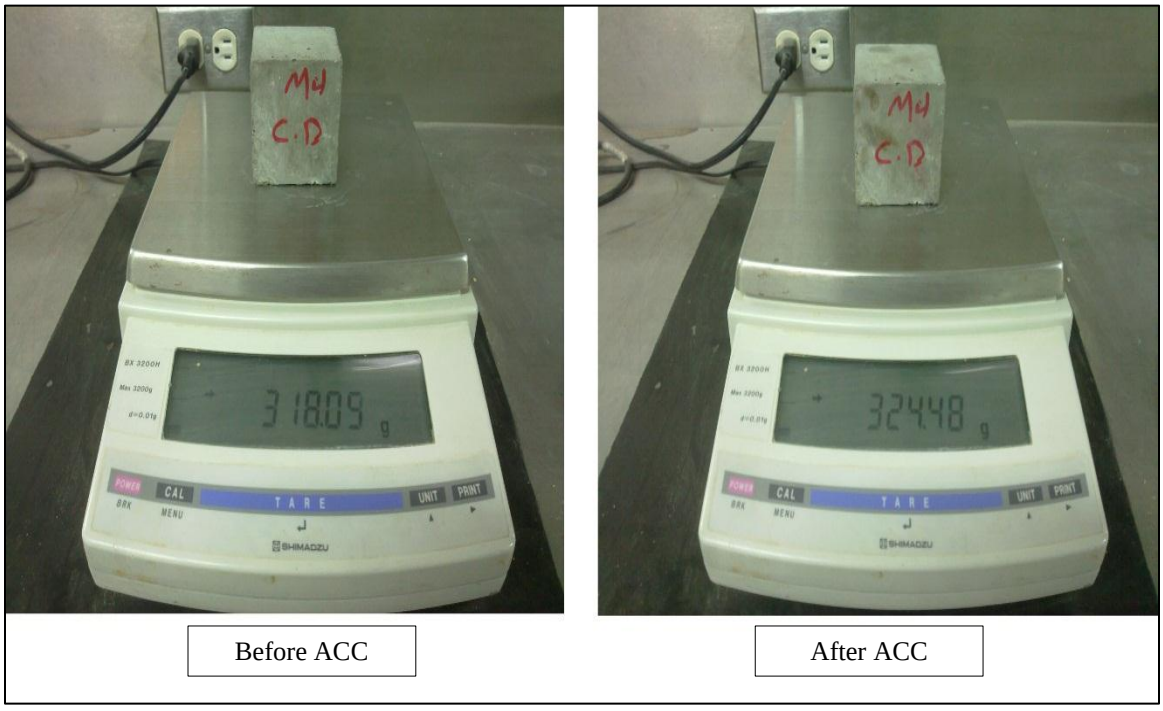

Figure 4.2: Weight gain test.

4.5 Tests for mechanical properties

4.5.1 Compressive Strength

Cubical concrete specimens of 50 mm size were used to determine the compressive strength of all the mixtures. Compressive strength was determined after 7, 14, 28 and 90 days in air for both ACC and burlap curing, according to ASTM C 39 [26]. An automatic compressive testing machine of hydraulic type (MATEST), as shown in Figure 4.3, was used to load the specimens with applied loading rate of 1 kN/s until crushing. The crushing load in kN was recorded and the compressive strength was calculated by dividing the failure load by the cube cross-sectional area (2500 mm^2).

Figure 4.3: Automatic compressive strength testing machine.

4.5.2 Splitting Tensile Strength

75 × 100 mm concrete cylinders were used to determine the splitting tensile strength of all the mixtures after 14-days of casting, according to ASTM C 496 [27]. The actual

dimensions of the specimens including height and diameter were measured before testing for more accuracy. As shown in Figure 4.4, an automatic compressive testing machine of hydraulic type (MATEST) was used for this test. The compressive loading rate was 1 kN/s. The load was applied through narrow bearing strips until the specimen failed by splitting into two halves.

Figure 4.4: Splitting tensile strength test preparation.

Procedures:

- Draw diametrical lines on the two ends of the specimen to ensure that they are on the same axial place.
- Note the dimensions of the specimen.

- Set the compression testing machine for the required range.
- Place the plywood bearing strip on the lower plate and place the specimen [28].
- Align the specimen so that the lines marked on the ends are vertical and centered over the bottom plate.
- Place the other strip above the specimen.
- Move the machine plate until upper plate touches the plywood strip.
- Apply the load with a constant rate of 1 kN/s.
- Note down the breaking load (P).

Calculations:

The splitting tensile strength is calculated using the formula

Tsp = $\frac{2P}{\pi D L}$ (MPa)

Where P = applied load at failure, N,

D = diameter of the specimen, mm, and

L = length of the specimen, mm.

4.5.3 Elastic Modulus

It is very important to check out the modulus of elasticity of each mixture in this research since this property has a considerable impact on deflection and prestress losses in prestressed elements [29]. The test has been conducted according to ASTM C 469 [30]. 75 × 100 mm concrete cylinder specimens were used to determine elastic modulus for all the mixtures after 14-days of casting. The specimens were tested using the same automatic testing machine used in compressive strength test. The compressive loading rate was 2 kN/s. The load and the corresponding deformation were recorded for each specimen using a data logger.

Installation of test equipment and specimens after testing is shown in Figure 4.5. As shown in Figure 4.5, the specimen was clamped in two circular steel frames by three screws on each frame, two Linear Variable Differential Transformer (LVDTs) were placed vertically on opposite sides to take into account any movement on specimen sides, one LVDT placed perpendicular to the movable plate of the compression machine to measure it's movement.

The linear deformations were captured by the LVDTs and the load was sensed by the load cell, which was placed under the specimen. LVDTs and load cell were connected to a data logger.

Figure 4.5: Elastic modulus test installation.

After collecting data from the data logger, the following formula was used to calculate the modulus of elasticity:

$$E = \frac{S_2 - S_1}{\epsilon_2 - 0.000050}$$

Where:

E = Modulus of elasticity, MPa,

S_2 = Stress corresponding to 40 % of ultimate load,

S_1 = Stress corresponding to a longitudinal strain, ϵ_1, of 50 millionths, MPa, and

ϵ_2 = Longitudinal strain produced by stress S_2.

4.6 Durability evaluation

4.6.1 Water permeability

Water penetration depth test was conducted according to DIN 1048 as an indicator of the water permeability. Cubical specimens of 100 mm size were used for this test. Three replicate specimens were prepared for each case. Figure 4.6 shows the apparatus used for performing water penetration depth tests under a defined pressure applied to the concrete specimens. The test was performed by clamping the specimen between two flanges with special circular gaskets. The water, under controlled 5 bars of pressure, was then applied to the surface of the concrete specimen. The specimens remained under constant water pressure for three days. After that, the specimens were split into two halves parallel to the water pressure direction. The penetration of water profile is then marked and an average penetration depth was determined.

Figure 4.6: Water permeability test.

4.6.2 Chloride permeability

The chloride permeability test is a rapid test performed to determine the electrical resistance of concrete against the penetration of chloride according to the standard method given in ASTM C 1202 [31].

The systematic procedure adopted for this test is as follows:

- A 50 mm thick concrete disk was cut out from the middle of the 75 x 150 mm cylindrical specimens prepared for this test.
- The cylindrical surface was coated with an epoxy to limit the penetration on the circular surfaces.
- Before testing, the disks were conditioned in vacuum desiccator for 4 hours and then left in water for about 18 hours.
- After that, rubber gaskets were fixed around the specimens. Then the specimens were placed in between the plexiglass measuring cells and water leakage test was then conducted before adding the solutions. Figure 4.7 shows the test set-up.
- 3%NaCl solution (w/w) was filled into the black head half-cell while the other half was filled with 0.3 N NaOH solution.
- A potential difference of 60 V DC was maintained across each cell holding the specimens and the total charge passed in coulombs was recorded at the end of the test, which continues for 6 hours.

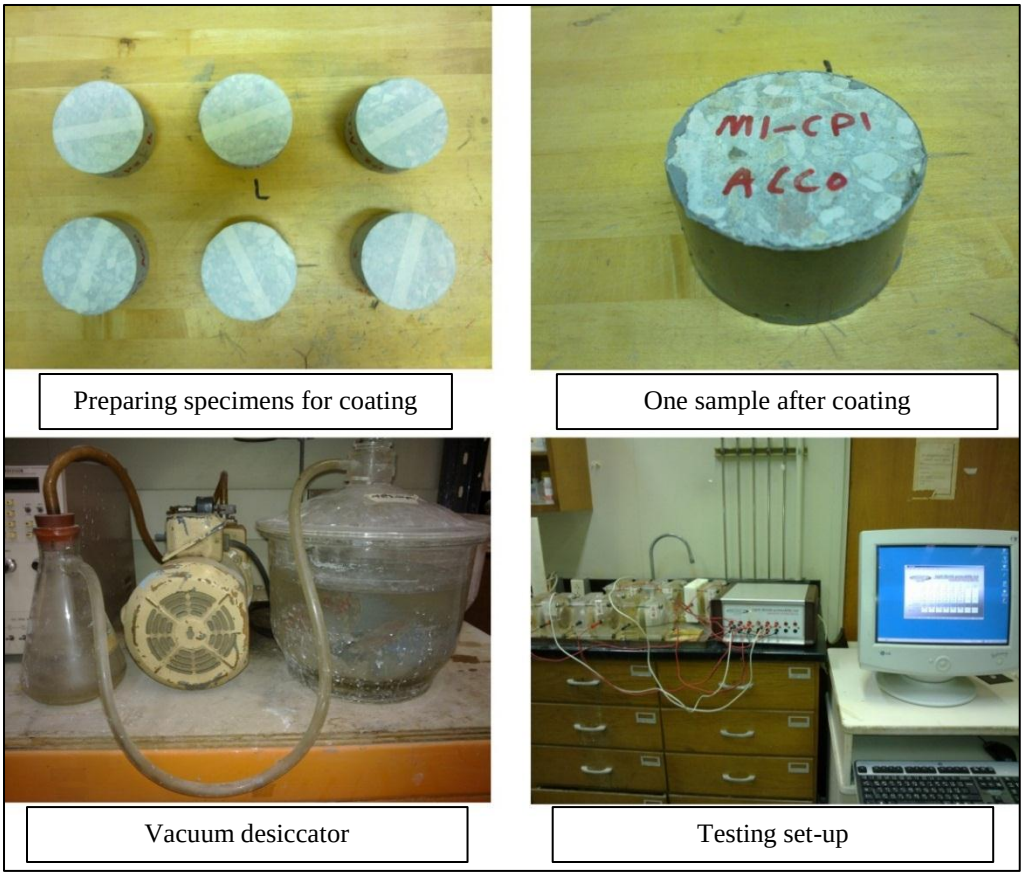

Figure 4.7: Chloride permeability test machine and sample preparation.

4.7 Drying shrinkage test

Drying shrinkage is defined as the contraction of a hardened concrete element due to the loss of capillary water. This shrinkage induces tensile stress, which may lead to cracking, internal warping, and external deflection, before the concrete is subjected to any kind of restrained [32].

The drying shrinkage test was conducted according to ASTM C 157 [33]. Three 50 × 50 × 250 mm concrete prisms were prepared for shrinkage test for each case of study. To achieve accuracy and reliability, a mechanical strain gauge, as shown in Figure 4.8, was used as strain measurement. Immediately after demolding, a pairs of stainless steel discs were fixed on the specimen surface using epoxy glue with center-to-center distance of 200 mm. The initial shrinkage readings before starting ACC and burlap curing were taken. Subsequently, monitoring of shrinkage was carried out throughout the entire curing regime (after ACC,

during burlap curing, and up to six months of air exposure). Figure 4.8 illustrates the mechanical gauge and shrinkage specimens. Shrinkage strain was calculated as follows:

$$\text{Strain} = \frac{change\ in\ length}{gauge\ length\ (200\ mm)}.$$

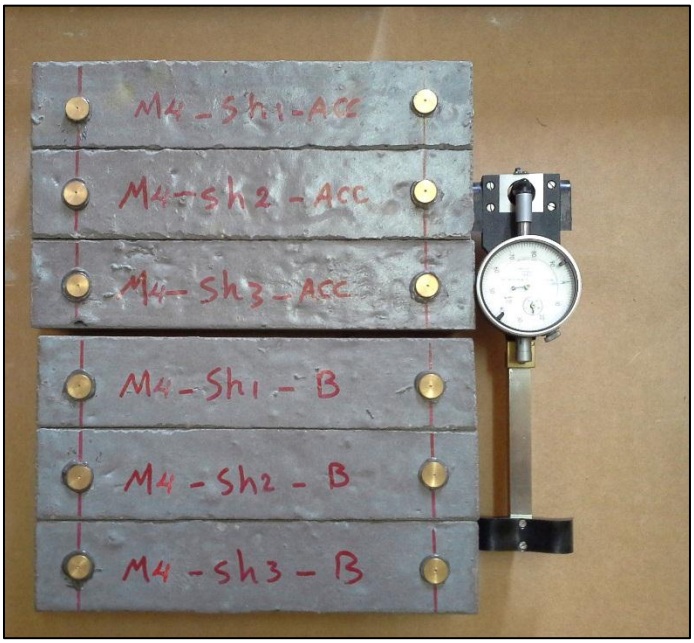

Figure 4.8: Drying shrinkage apparatus and specimens.

4.8 Physico-chemical tests

4.8.1 Scanning electron microscopy (SEM)

Scanning electron microscopy is one of the most advanced technical tools that can be used versatility to examine and analyze concrete microstructure. The high resolution achieved by using SEM, which reaches to 2.5 nm, is the source of importance [34]. Furthermore, SEM can be used to determine the elemental composition of the tested material [34]. In this research, several samples distributed all over the mixtures were tested. After finishing the curing and crushing of concrete specimens, small portions were taken from the surficial layers of the crushed specimens, kept in a plastic bag, and placed inside a desiccator until testing. Figure 4.9 shows sample preparation and the set-up of the SEM used in this research.

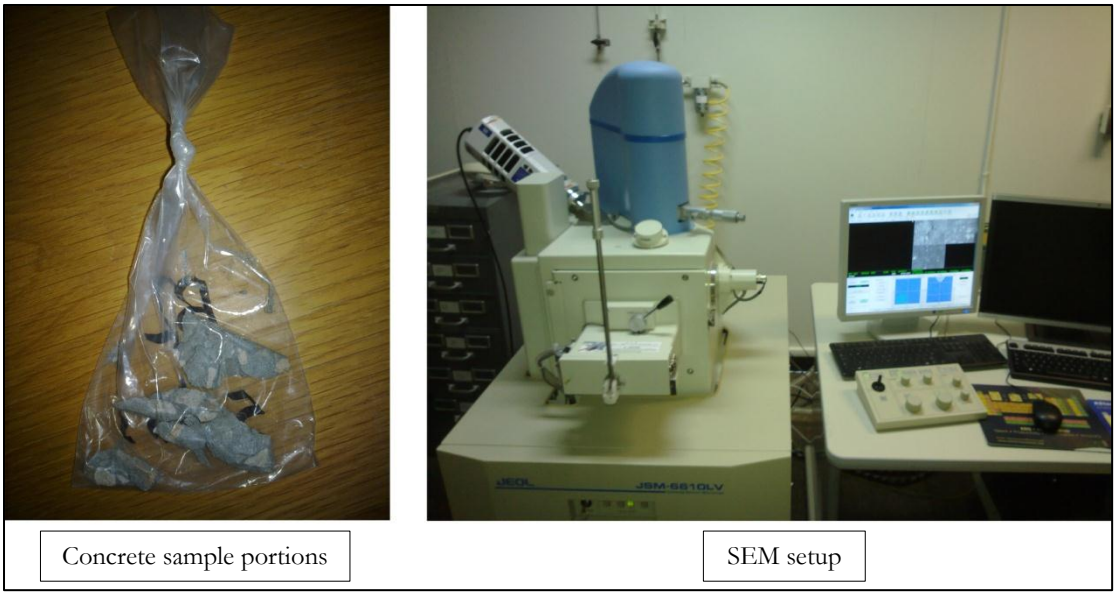

Figure 4.9: SEM, sample preparation and test setup.

4.8.2 X-ray diffraction (XRD)

X-ray Diffraction is an analytical and semi-quantative technique used primary to identify and characterize mineralogical composition based on their diffraction pattern. Every mineral has a unique ID, which is made up of its specific angles [35].

XRD has three primary uses in today's research. First and foremost, it is used to identify individual mineral samples and their corresponding characteristics. Secondly, it allows identification of specific mineral components within mixed clay or soil samples. Thirdly, it provides an insight of unit cell dimensions, which is the distance between the inner protons and neutrons [36].

XRD has many advantages. Firstly, this process is very rapid, usually taking less than twenty minutes. The results are unambiguous, with very little error. The preparation is very minimal, just sample collection and cleaning of the machine. The XRD machines are common and widely available around the world. The final interpretation is very straightforward allowing for easily replicated results [36].

In this research, several samples distributed all over the mixtures were tested. After finishing the curing and crushing of concrete specimens, small portions were taken from

the surficial layers of the crushed specimens and then the aggregate particles were removed. The rest have been ground using the shown grinder in Figure 4.10. After that, the concrete powder was kept in a plastic bag and placed inside a desiccator until testing. Figure 4.10 shows sample preparation and the set-up of the XRD used in this research.

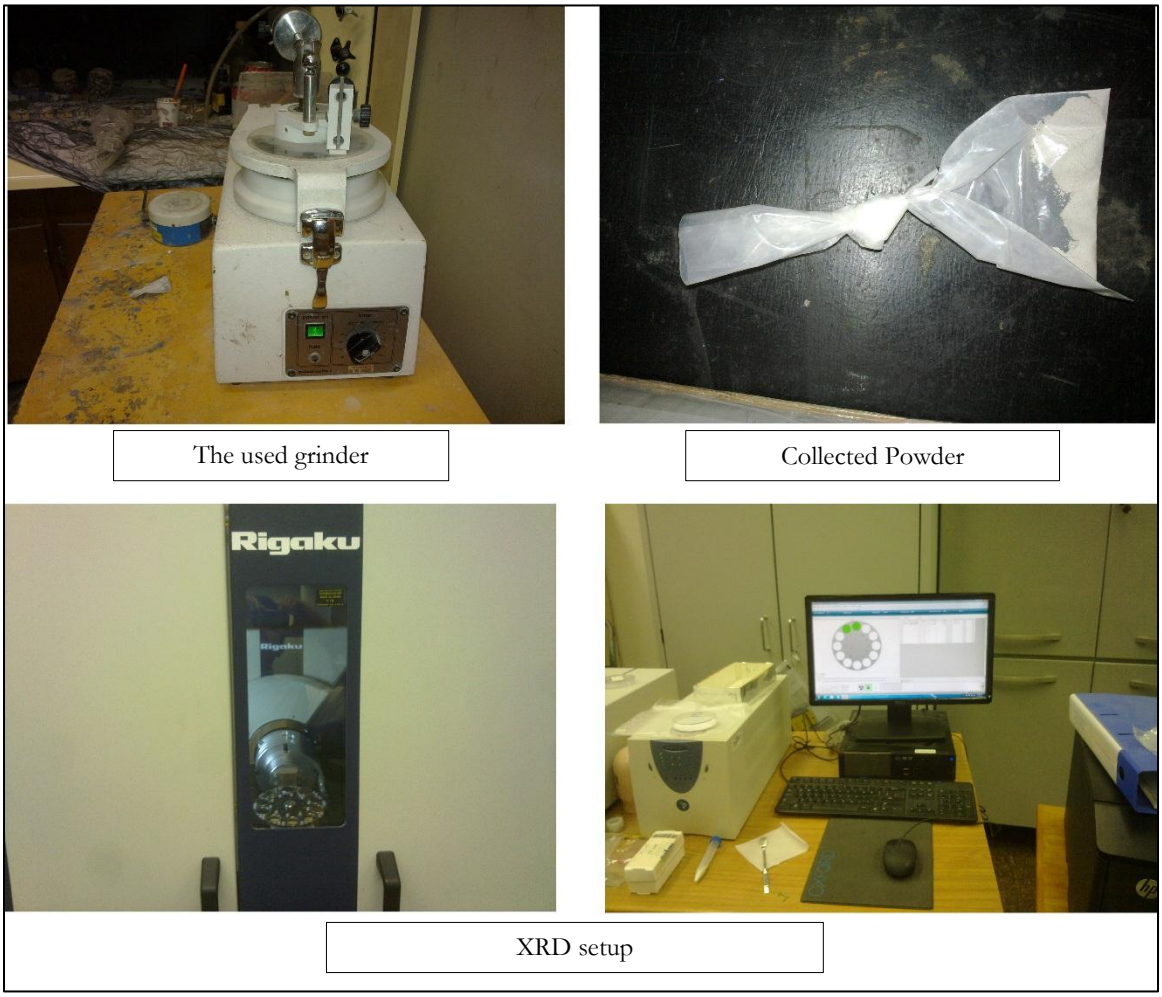

Figure 4.10: XRD, sample preparation and test setup.

CHAPTER 5

RESULTS AND DISCUSSION

In this chapter, the test results, collected through the experimental work conducted according to the methodology as presented in previous chapters, were compiled. The preliminary test results were used to select the optimal ACC regime. Then the test results pertaining to four different concrete mixtures cured using the optimal ACC regime was used to evaluate its effectiveness on the performance of the concrete mixtures.

5.1 Selection of Optimal Pressure and Exposure Duration for ACC

5.1.1 Effect of Pressure and Exposure Duration of ACC on Evolution of Compressive strength

The compressive strength of normal concrete mixture meeting the requirements of standard initial strength (16 ± 2 MPa) and cured with ACC regime (i.e., ACC using 60 different combinations of *pressure* and *CO_2 exposure duration*) are shown in Table 5.1. Table 5.1 contains 10 different exposure durations to CO_2 gas starting from 1 hour up to 10 hours and six different pressures starting from 10 hours up to 60 psi. Each value of compressive strength in the table represents an average of four specimens.

Table 5.1: Compressive strength results to evaluate the optimum pressure and duration.

Batch ID	Initial strength after demoulding and before ACC (MPa)	Pressure (psi)	Compressive strength (MPa) after ACC									
			1 h.	2 h.	3 h.	4 h.	5 h.	6 h.	7 h.	8 h.	9 h.	10 h.
B1	14.1	**10**	16.0	17.9	19.1	19.1	22.0	22.8	23.1	23.8	25.2	25.0
B2	14.4	**20**	15.5	16.8	17.5	20.5	22.6	23.3	24.1	25.9	27.5	25.4
B3	15.3	**30**	18.1	20.2	19.8	22.3	24.5	24.0	22.9	23.6	22.6	24.1
B4	14.4	**40**	17.0	20.4	20.4	20.8	22.9	25.7	23.7	26.2	24.9	26.5
B5	15.9	**50**	18.0	20.1	22.2	22.4	24.2	25.8	26.9	28.0	29.1	25.8
B6	14.3	**60**	18.8	18.3	21.1	24.9	24.6	23.4	26.5	29.0	30.4	30.3

The results presented in Table 5.1 were plotted to see the effect of pressure and duration of ACC, as shown in Figure 5.1. Generally, an increase in compressive strength was noted at all ACC pressures. However, a common behavior noticed is of somewhat periodic nature, as evident from the compressive strength evolution curves, rather than an expected steady trend of strength gain. This periodic behavior is most pronounced at higher pressure of 60 psi, and seems less pronounced at low pressure of 10 and 20 psi. Given the fact that retrieval specimens from the ACC chamber was done at intervals as the time progressed, one may attempt to associate the periodic trend to a possible hindrance to carbonation offered by the air allowed temporarily in the ACC chamber in the brief course of the periodic retrieval specimens. However, the following major argument offers an opposing view to this explanation for the seemingly anomalous trend.

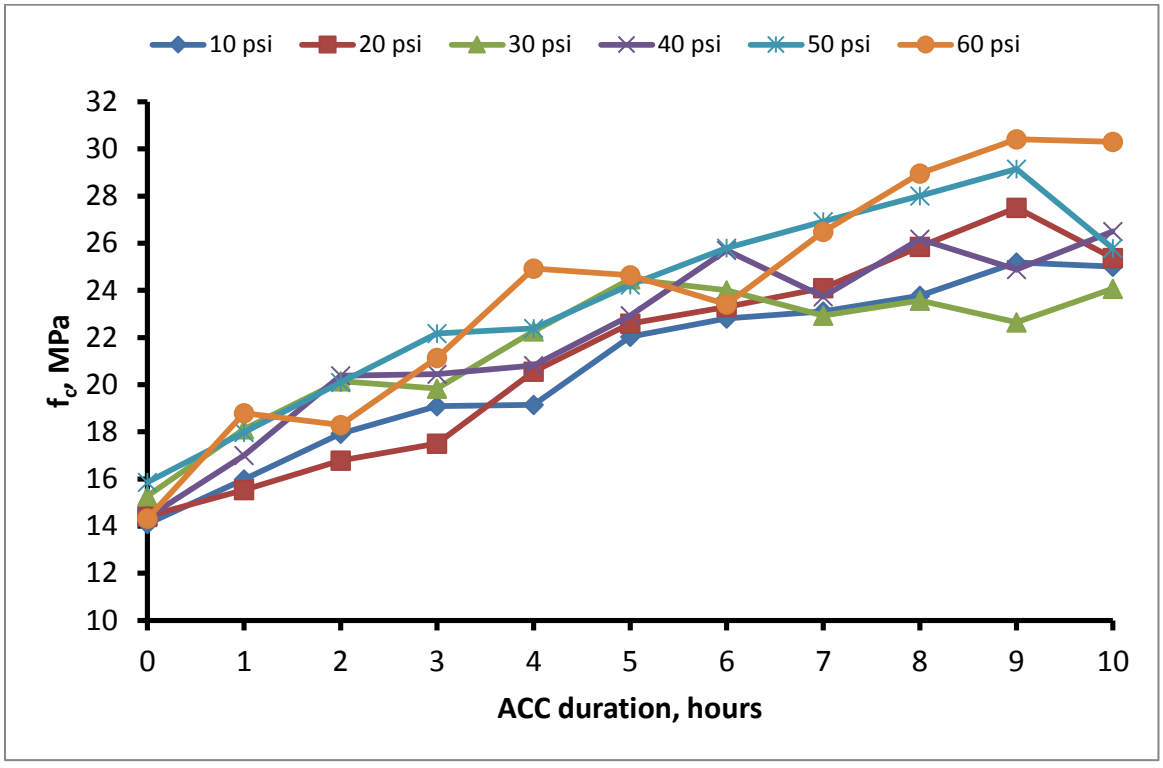

Figure 5.1: Compression strength versus different pressures and durations.

Referring to Figure 5.1, the strength drops did not occur at hourly intervals, against the hourly temporary allowance of air in the ACC chamber. In other words, the strength

evolution periods, though irregular, are not exactly one hour, while the ACC interruption interval was a constant one hour. The argument, against associating the periodic strength evolution curves with the periodic ACC interruption, can best be supported by the 60 psi curve, followed by the other curves. It can subsequently be argued that the reported periodic trend may not necessarily be connected with the temporary allowance of air in the ACC chamber. This will finally lead to a conclusion that the periodic strength gain trend is characteristic of the ACC process itself. In this line of thought, an explanation for the periodic strength evolution will be proposed shortly. Also, it can be observed from Figure 5.1 that ACC at 60 psi resulted into the highest strength gain. Although, the strength gain due to ACC at 60 psi showed the most pronounced effect of periodic fluctuations, the 10-hour strength is the highest (around 30 MPa), while its initial strength was on the lower side of the distribution (around 14 MPa). On the extreme end, the low ACC pressures of 10 to 40 psi did not produce comparable strength gain relative to increased pressure of ACC. Depending on the required compressive strength, Figure 5.1 could be used to determine the appropriate pressure and duration.

Figure 5.2 depicts the compressive strength development with varying ACC pressures. The importance of these strength evolution rate curves lies in their ability to highlight the manner in which additional strength increase was attained, in the course of ACC, on hourly basis. It is apparent from the data in Figure 5.2 that regardless of the ACC pressure, the overall outlook is a general reduction in the rate of additional strength gain, as indicated by the bounding dashed lines with negative slopes. More specifically, the periodic fluctuations in strength observed in Figure 5.1 can be better visualized in these rate curves (Figure 5.2).

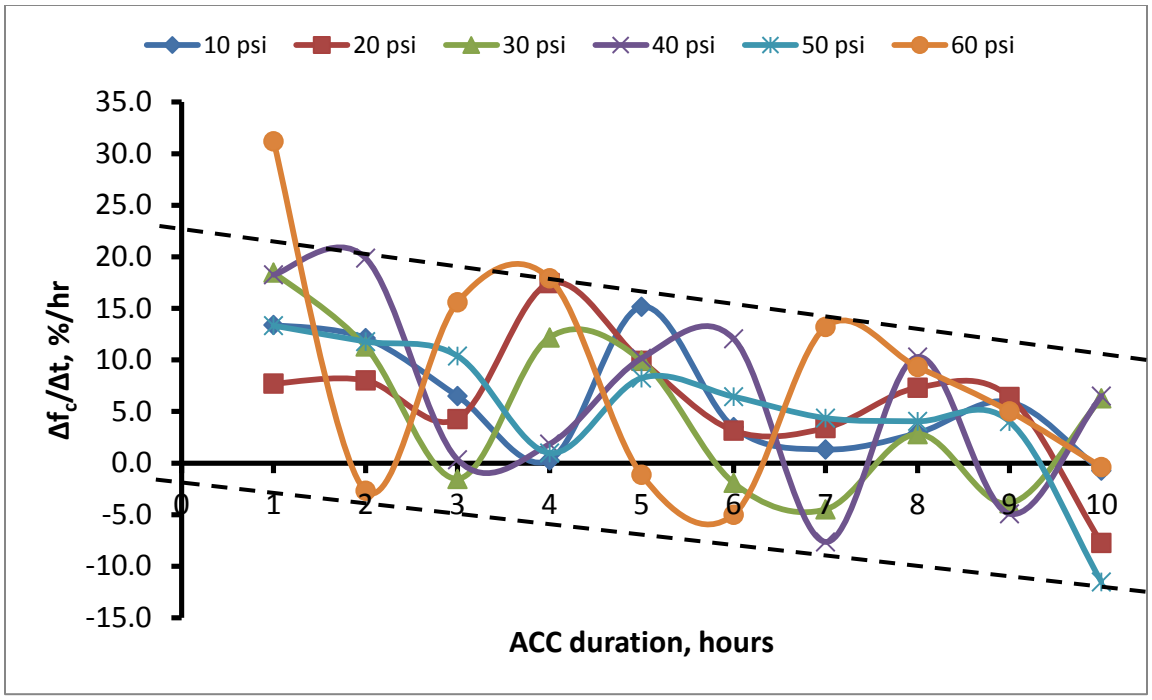

Figure 5.2: Evolution rate of compressive strength.

Since the periodic strength fluctuations is more pronounced at higher pressures, it may be inferred from Figure 5.2 that this phenomenon results from periodic loss in structural fitness of the previously formed $CaCO_3$-CSH structures, which helps in supporting the microstructural stress threshold via intra-capillary pore densification. This loss of structural fitness results from mechanical disruption of the young structural gels because of continuous bearing of ACC pressure. When this happens, the instantaneous strength becomes lower than expected or even lower than that obtained at the previous ACC duration before the structural disruption of the $Ca(OH)_2$ and/or C-S-H. This so-called structural disruption would lead to exposure of reactive primary hydration products that might be previously masked by dense layers of $CaCO_3$ gels, a situation that would have receded further carbonation in the absence of the disturbance. After further ACC, new $CaCO_3$-CSH structures formed would again prop up the microstructural strength. At this stage, the previously disrupted $CaCO_3$-CSH structures get 'repaired' by the formation of new structures around the old units, so that the general microscopic repair process leads to additional strength at macroscopic level over what was available before the previous disruption of the $CaCO_3$-CSH structures. The disrupt-repair cycle would then continue to

produce the periodic strength evolution behavior. Figure 5.3 shows the sequence of disrupt-repair cycle of CaCO3-CSH structures.

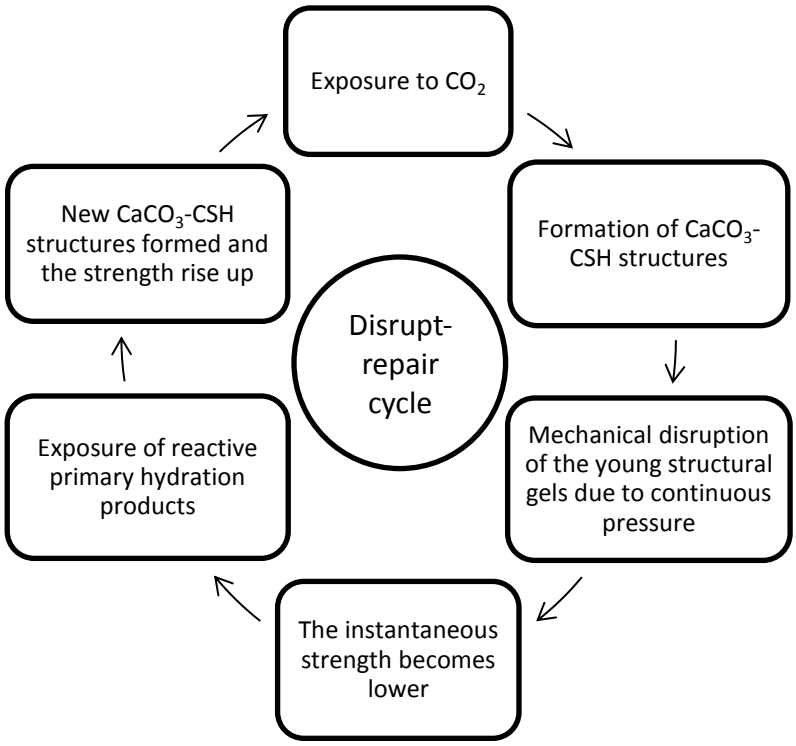

Figure 5.3: Disrupt-repair cycle of $CaCO_3$-CSH structures.

Many disrupt-repair cycles lead to more densification to a certain depth from the surface, which is expected to depend on the ACC pressure for a given concrete mixture, so that the rate of advancement of CO_2 front into the body of the concrete declines and subsequently the strength gain slows down completely, as observed in Figure 5.1 at about 9 to 10 hours of ACC. This observation conforms to the submission made by Kashef-Haghighi (2013) [7], who attributed the hindrance in continuous CO_2 uptake to the formation of the layer of $CaCO_3$ during carbonation because the formed layer of $CaCO_3$ reduces the available reactive surface area of cement for carbonation.

On a general note, for the concrete mixture considered in this study, Figure 5.1 and Figure 5.2 show that ACC at a pressure of 60 psi for a period of 10 hours is likely to produce the best benefit of ACC, if the carbonation front is not too deep.

5.1.2 Weight gain due to ACC at different pressures and durations

The accumulated weight gains related to the different exposure durations and pressures are shown in Table 5.2. Each value of weight gain in the Table 5.2 represents an average of four specimens.

Table 5.2: Weight gain results to evaluate the optimum pressure and duration.

Batch ID	Maintained pressure (psi)	Weight gain as % of cement based on exposure duration to CO_2									
		1 h.	2 h.	3 h.	4 h.	5 h.	6 h.	7 h.	8 h.	9 h.	10 h.
B1	**10**	1.5	1.8	1.6	2.6	1.8	2.4	2.6	3.1	2.9	4.8
B2	**20**	2.0	2.2	2.2	2.4	1.8	2.9	2.9	2.8	2.7	3.3
B3	**30**	0.8	1.6	1.8	2.2	2.2	2.4	2.5	2.9	3.4	4.0
B4	**40**	1.7	1.7	2.1	2.6	2.8	2.4	2.9	3.1	2.8	3.7
B5	**50**	2.3	3.1	3.3	3.3	3.7	3.8	3.8	4.2	4.4	4.7
B6	**60**	1.7	2.7	3.6	4.3	4.8	4.8	5.0	5.4	6.1	5.8

The effectiveness of ACC can be directly assessed by the actual amount of CO_2 that has been successfully sequestrated into concrete. This is usually expressed in terms of the net uptake of CO_2 as a percentage of dry binder [1], [10], [11]. The actual mass of a carbonated concrete element excludes the amount of lost water to the exothermic reaction that takes place during the course of ACC [1]. Therefore, this lost water needs to be added to the actual mass of the carbonated concrete element. The general expression for CO_2 uptake is given as:

$$CO_2\ uptake\ (\%) = \frac{Mass_{post-CO_2} + Mass_{lost\ water} - Mass_{pre-CO_2}}{Mass_{binder}}$$

Figure 5.4 shows the progress of CO_2 uptake in terms of weight gain, expressed as percentage of cement, as ACC progressed at various pressures and durations. As stated earlier, the quantity of water lost during the course of ACC needs to be taken care of in the calculation. However, the experimental procedure employed in this study did not permit easy determination of the water loss. For each ACC pressure, all the specimens for the entire 10-hour duration were stocked together in the carbonation chamber, while a set of specimens were retrieved on hourly basis for testing, leaving others for longer testing duration in the chamber for further CO_2 exposure and the pressure restored. Therefore, the

results presented in Figure 5.4 do not account for the carbonation-induced dehydration of the specimens. As such, the values presented have been grossly underestimated. Nevertheless, the evolution of weight gain presented in Figure 5.4 is still useful for comparative assessment of the effect of ACC duration and pressure.

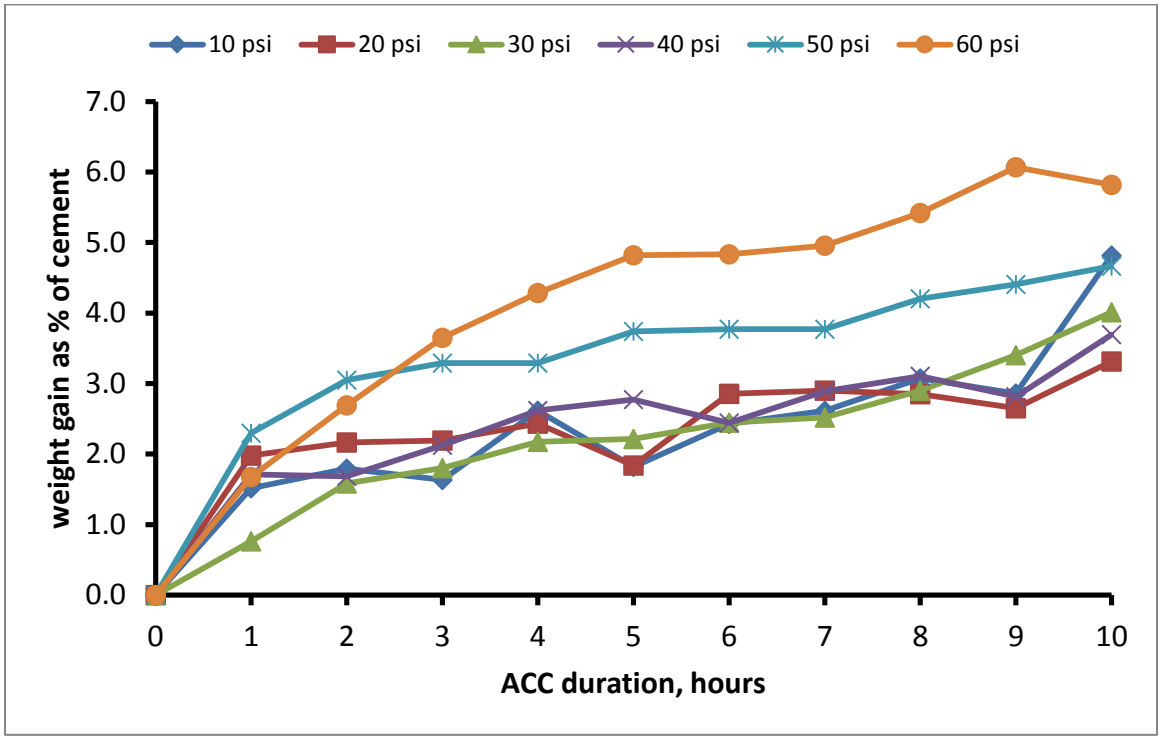

Figure 5.4: Evolution of CO_2 uptake in terms of weight gain as percentage of cement.

With reference to Figure 5.4, for all ACC pressures, the weight gain of ACC-exposed concrete specimens continued almost throughout the whole ACC duration of 10 hours, but at diminishing rates, which confirms the proportionality relationship between strength and weight gain. Apart from the 10 psi ACC pressure, about three-quarter of the total mass gain after 10-hour had been attained in 4 hours. Moreover, it can be noticed that the diminishing rate of weight gain as the ACC progressed was more pronounced at 10 to 40 psi ACC pressures, while the higher pressures exhibited the diminishing rate behavior to a lesser degree. Considering the ultimate weight gain at 10 hours of ACC, 50-psi pressure imparted about 150% more weight gain than the low pressures (10 to 40 psi), while 60 psi caused about 200% weight gain at low ACC pressures (coming out with a total increase of 6% of

cement mass). Therefore, considering the maximum CO_2 sequestration potential, ACC at 60 psi exhibited the best performance at nearly all durations of ACC.

5.1.3 Carbonation depth

Figure 5.5 shows a typical phenolphthalein stained concrete fractured surface. After ACC, the specimen splitted into two equal fractions and then the phenolphthalein solution sprayed through all the inner surface of the fractions.

Figure 5.5: Typical phenolphthalein stained concrete fractured surface.

The measured carbonation depth, as indicated by the thin layer of discolored portion towards the concrete surface, was ≤ 2.0 mm for all ACC pressures. Irregular carbonated profile was noticed along the outer layer of the specimens. This profile tends to have more penetration depth around aggregate particles due to heterogeneity. Although the carbonation profile depth was irregular, the low average depth of 2 mm will not be a significant threat of de-alkalization-induced corrosion of reinforcement steel bars embedded in concrete with a usual minimum clear cover of 20 mm from the surface. This emphasizes what was observed by Rostami et al. [11], who stated that the reduction in pH does not usually occur beyond a negligible depth below the surface exposed to ACC and the reinforced concrete can be cured using ACC.

5.1.4 Statistical study

The pressure inside the chamber and the exposure duration to CO_2 gas are the most important factors affecting the results. To determine the significance of the factors in ACC process, two-factor without replication ANOVA was conducted on both compressive strength and weight gain rates. The significance level was considered equal to 5%. Table 5.3 and Table 5.4 show the detailed analysis for compressive strength gain and weight gain rates, respectively.

Table 5.3: ANOVA for compressive strength gain rate.

Source of Variation	*SS*	*df*	*MS*	*F*	*P-value*	*F crit*
Rows (pressures)	73.484146	5	14.696829	0.3127001	0.9027694	2.4220855
Columns (hours)	1482.8724	9	164.76359	3.5056268	0.00233	2.0957551
Error	2114.9889	45	46.999753			
Total	3671.3454	59				

Table 5.4: ANOVA for weight gain rate.

Source of Variation	*SS*	*df*	*MS*	*F*	*P-value*	*F crit*
Rows (pressures)	0.4086656	5	0.0817331	0.3825293	0.8581248	2.4220855
Columns (hours)	12.22734	9	1.3585933	6.3585211	9.179E-06	2.0957551
Error	9.6149243	45	0.213665			
Total	22.25093	59				

It is very clear that the exposure duration factor controls the curing process in both compressive strength and weight gain cases since P-value was less than 0.05. Similarity in behavior may support the proportionality relationship between strength and weight gain.

5.2 Weight gain due to optimum ACC of different concrete mixtures

As stated earlier under the detailed study, the optimized ACC using 60-psi chamber pressure and 10 hours of exposure duration was conducted for all the four mixtures studied in the present work. The weight gain was calculated after subjecting 20 cubical specimens

to ACC for each of the four mixtures. The specimens were weighed before and after ACC to find out the average CO_2 weight gain of each mixture, expressed as percentage weight gain by mass of cement. Figure 5.6 shows the weight gain for the four concrete mixtures.

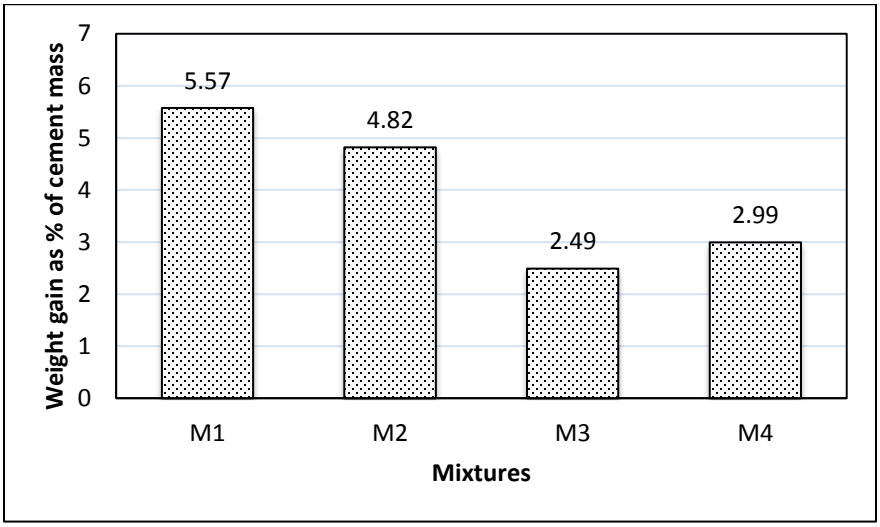

Figure 5.6: Weight gain (as percentage of cement mass) after applying optimal ACC.

The normal concrete mixtures (M1 and M2) show relatively higher weight gain due to ACC than the SCC mixtures (M3 and M4). This is because of the fact that the mixtures M3 and M4 have denser microstructure due to use of lower water/binder ratio of 0.30 and higher cementitious materials content of 500 kg/m^3 than that of the mixtures M1 and M2, which had a water/binder ratio of 0.45 and a cementitious materials content of 375 kg/m^3. It can be seen from Figure 5.6 that the mixtures M1 and M2 having same water/binder ratio and cementitious materials have a little bit different weight gain. This is because of the different amount of $Ca(OH)_2$ available for carbonation due to different compositions of cementitious materials (M1 with only Portland cement and M2 with the blend of 80% Portland cement and 20% fly ash). The reason behind difference in weight gains in the mixtures M3 and M4 is same.

5.3 Carbonation depth due to optimum ACC of different concrete mixtures

After subjecting specimens (belonging to all the four mixtures) to optimal ACC using 60-psi chamber pressure and 10 hours of exposure duration, carbonation depths were

determined using the same procedures as illustrated in Section 5.1.3. Figure 5.7 shows the plots of carbonation depths measured for all the four mixtures.

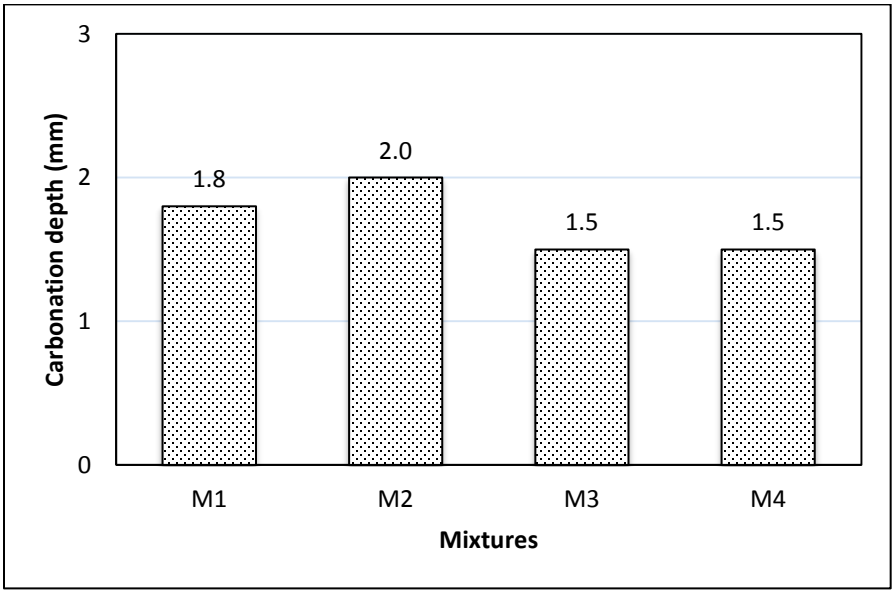

Figure 5.7: Carbonation depth after applying optimal ACC

It can be observed from Figure 5.7 that the carbonation depth was ≤ 2.0 mm for all mixtures. However, carbonation depths in self-compacting concrete mixtures (M3 and M4) were lower than that of normal concretes (M1 and M2). This is because of the dense microstructure of mixtures M3 and M4 formed due to lower water/binder ratio and higher amount of cementitious materials. It can be seen further from Figure 5.7 that the mixtures M1 and M2 having same water/binder ratio and cementitious materials have a little bit different carbonation depths. This is because of different amount of $Ca(OH)_2$ available for carbonation due to different compositions of cementitious materials (M1 with only Portland cement and M2 with the blend of 80% Portland cement and 20% fly ash). The mixtures M3 and M4 have same carbonation depth as 1.5 mm.

5.4 Evolution of compressive strength

The compressive strength results of all mixtures for both ACC and burlap curing are shown in Table 5.5 and Table 5.6, respectively. For ACC curing regime, the compressive strength test was conducted at different stages as follows: (i) directly after 10 hours of ACC curing, (ii) after 7, 14, 28 and 90 days exposure in air with laboratory conditions following the 10

hours of ACC curing. For burlap curing regime, the specimens were crushed (i) after 7 days of burlap curing, (ii) after 7, 14, 28 and 90 days of exposure in air with lab conditions following 7 days of burlap curing. Each value in the two tables represents an average of 4 specimens.

Table 5.5: Summary of compressive strength results for ACC specimens for all mixtures.

Mixture ID	Compressive Strength (MPa)					
	Initial strength at 18 hours (immediately after demolding)	Directly after ACC curing for 10 hours	Air curing (days) after ACC			
			7	14	28	90
M1	14.99	26.87	43.87	45.57	47.12	48.2
M2	17.70	23.8	37.8	40.84	47.11	49.69
M3	19.36	31.63	51.69	52.37	54.66	55.66
M4	25.91	36.54	70.17	73.29	75.69	78.51

Table 5.6: Summary of compressive strength results for burlap specimens for all mixtures.

Mixture ID	Compressive Strength (MPa)					
	Initial strength at 18 hours (immediately after demolding)	Directly after Burlap curing for 7 days	Air curing (days) after burlap curing			
			7	14	28	90
M1	14.99	38.46	50.1	53.35	54.83	55.57
M2	17.70	39.47	43.27	46.6	51.63	52.08
M3	19.36	53.54	61.67	64.69	68.8	70.57
M4	25.91	63.35	73.72	81.41	84.06	85.57

From Table 5.5, the increments in strength due to 10 hours of ACC were calculated as: 79, 63, 41, and 34%, respectively, in cases of M1 (using plain cement without mineral admixtures), M3 (using LSP as admixture, which had significant amount of silica), M4 (using LSP and SF as mineral admixtures, which together contributed high amount of silica), and M2 (using FA as admixture, which contributed high amount of silica). The increase in the strength of concrete mixtures due to carbonation may be attributed to the ability of carbonation to make the concrete surface harder due to the formation of $CaCO_3$. However, these results indicate that the effectiveness of ACC in achieving strength higher in the absence of silica from a mineral admixture. This is because of the fact that the

significant amount of $Ca(OH)_2$ is consumed if silica is added as mineral admixture, leaving behind a lesser amount of $Ca(OH)_2$ available for carbonation. The strength development is therefore lesser due to a lesser degree of carbonation achieved during the period of 10 hours.

5.4.1 M1: Plain Cement-NVC

Figure 5.8 shows the compressive strength for the mixture M1. As can be seen from Figure 5.8, the ACC specimens achieved a higher compressive strength during first 7 days of air exposure. Around 63% increase in the compressive strength due to the air curing for 7 days after ACC was recorded. However, very little benefit of air curing after ACC was observed after 7 days of air exposure, as evident from the almost flat portion of strength evolution curve shown in Figure 5.8. A similar trend of strength evolution was observed for burlap-cured specimens. An increase of about 30% in compressive strength was noted when burlap-cured specimens were exposed to air for 7 days. Like the case of ACC, the benefit of air exposure after burlap curing is not significant beyond 7 days of air exposure.

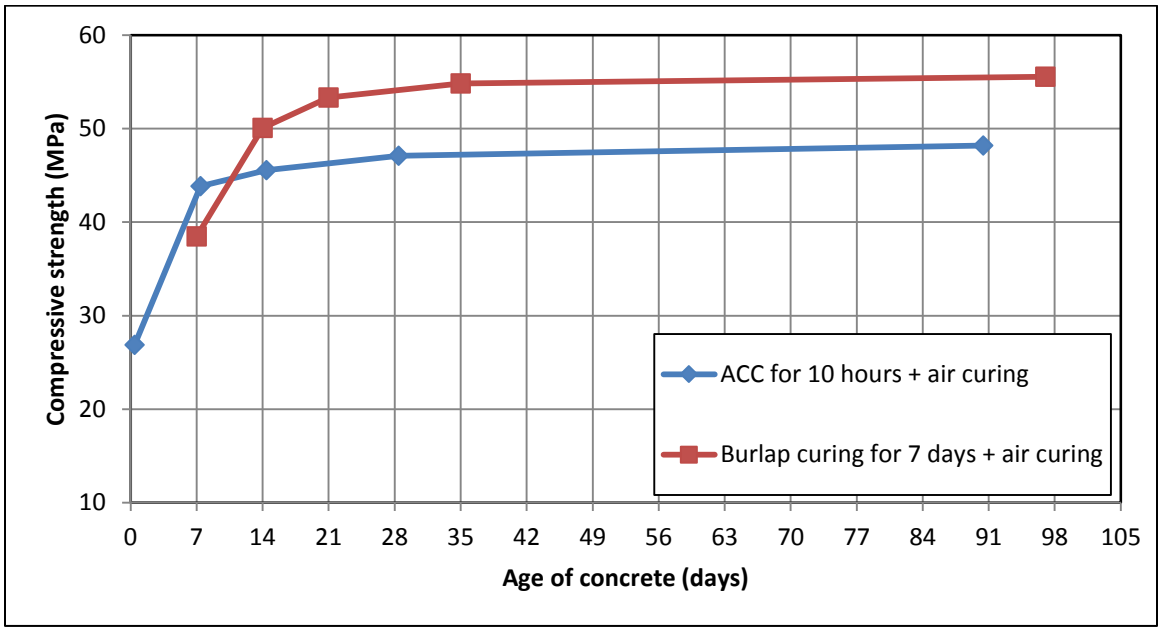

Figure 5.8: Post carbonation effect on compressive strength of M1.

It is important to note from Figure 5.8 that the strength of ACC specimens after 7 days in air is found to be about 14% more than the strength of specimens after 7 days of burlap curing. However, the strength of burlap-cured specimens kept in air for 7 days was found

to be around 10% more than the strength of ACC specimens kept in air for 14 days. This can be explained by the fact that the carbonated layer around the surface of the ACC specimen significantly reduces the evaporation of the moisture from the core of the specimens, which results in a faster rate of hydration until the most of the moisture content consumed resulting into gain of strength at a faster rate. On contrary, in the specimens subjected to burlap curing for 7 days, the rate of strength gain is slower than that of ACC specimens exposed to air for first 7 days due to slower rate of hydration. Because of slow rate of hydration during burlap period, the amount of residual moisture available in the pores of burlap specimens is more than that of ACC specimens (because ACC specimens consumed almost entire pore water in hydration during first 7 days of air exposure). Therefore, the strength of burlap specimens after exposing to the air is more than that of the ACC specimens.

It can be further noted that the difference in the strength of ACC and burlap specimens is almost constant (by around 15%) during the long-term air exposure. Therefore, it may be concluded that the difference in the strength of ACC and burlap-cured specimens will be 15% during the service life of concrete. It is worth mentioning that the ACC concrete has achieved a strength of 27 MPa only after 10 hours of carbonation making the carbonation-cured concrete able to handle only after 10 hours of curing.

5.4.2 M2: Cement and FA-NVC

Figure 5.9 shows the plot of evolution of compressive strength of the concrete mixture M2, in which 20% of cement was replaced by fly ash. It can be seen from Figure 5.9 that the ACC specimens exposed to air for the first 7 days achieved 59% more strength than that recorded immediately after the ACC. The increase in the strength of burlap-cured specimens after first 7 days of air exposure was only about 10%. However, unlike the case of mixture M1 made of only cement as binder, the strength of ACC specimens of the mixture M2 after exposure to air for 7 days is almost similar to that of the specimens of mixture M2 cured for 7 days using burlap. This is because of relatively lower degree carbonation achieved for mixture M2 due to availability of lower amount of $Ca(OH)_2$. The mixture M2 having 20% less cement due to replacement by fly ash, produced lower quantity of $Ca(OH)_2$. This relatively lower amount of $Ca(OH)_2$ was further reduced in

secondary hydration with silica from the admixed fly ash. Due to the lower degree of carbonation, the enhancement of strength owing to the increased surface hardness was relatively lower giving lower strength.

Unlike the case of mixture M1 where the rate of strength gain became almost negligible after 7 days of air exposure of both ACC as well as burlap specimens, the rate of strength gain for both types of specimens in case of mixture M2 was considerable up to 28 days of air exposure, as can be seen from Figure 5.9. This is because of slow rate of hydration due to addition of fly ash to mixture M2, which involved secondary hydration.

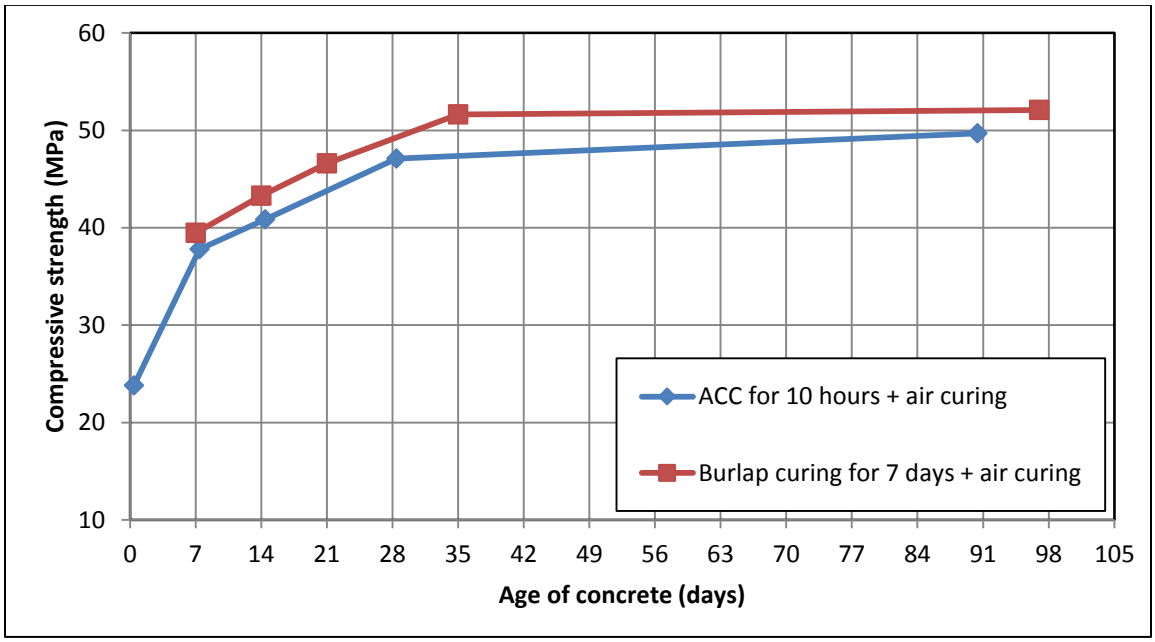

Figure 5.9: Post carbonation effect on compressive strength of M2.

It can be finally noted from Figure 5.9 that the difference in the strength of ACC and burlap specimens is almost constant (by around 5%) during the long-term air exposure. Therefore, it may be concluded that the difference in the strength of ACC and burlap-cured specimens of mixture M2 will be only 5% during the service life of concrete. It can be noted that the ACC concrete has achieved a strength of 24 MPa only after 10 hours of carbonation making the carbonation-cured concrete able to handle only after 10 hours of curing.

5.4.3 M3: SCC using LSP as Mineral Filler

Figure 5.10 shows the trend of development of compressive strength of the SCC mixture M3, which had 20% LSP and 80% cement by mass of the total cementitious materials. It can be observed from Figure 5.10 that the ACC specimens exposed to air for the first 7 days achieved 63% more strength than that recorded immediately after the ACC. However, like mixture M1, there is very small increase in strength after 7 days of air exposure. In case of burlap-cured specimens, the increase in strength after 7 days in air was significant (15% increase after 7 days in air following the burlap curing) and after that, strength increased slightly. The reason behind the evolution of strength of the mixture M3 being similar to that of the mixture M1 can be attributed to the fact that the blend of Portland cement and LSP has almost similar composition as the Portland cement alone. In mixtures M1 and M3, more degree of carbonation during 10 hours of exposure was achieved because of the availability of more amount of $Ca(OH)_2$ in absence of secondary hydration in case of M1 and very weak secondary hydration between $Ca(OH)_2$ and little amount of silica from limestone powder in case of M3. Higher degree of carbonation enabled the formation of dense surfaces that reduced evaporation of water from inside the concrete. The reduced evaporation made water to be available inside concrete to achieve almost complete hydration during first 7 days of air exposure.

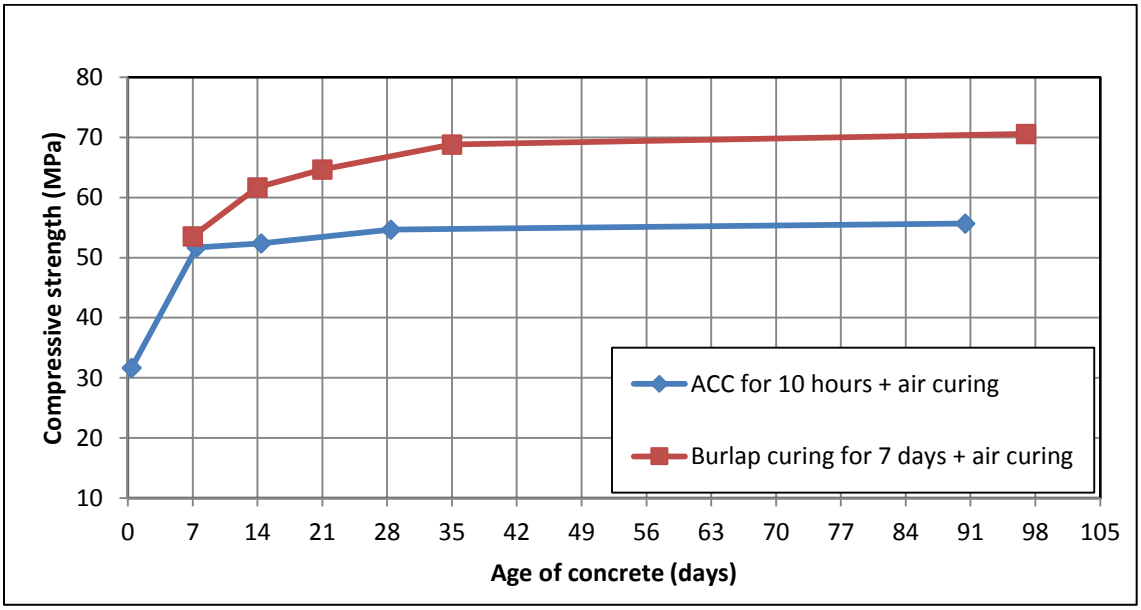

Figure 5.10: Post carbonation effect on compressive strength of M3.

It can be concluded from Figure 5.10 that the difference in the strength of ACC and burlap specimens is almost constant (by around 26%) during the long-term air exposure. Therefore, it may be concluded that the difference in the strength of ACC and burlap-cured specimens of mixture M3 will be 26% during the service life of concrete. However, the ACC concrete has achieved a strength of 32 MPa only after 10 hours of carbonation making the carbonation-cured concrete able to handle only after 10 hours of curing.

5.4.4 M4: SCC using LSP and SF as Mineral Fillers

Figure 5.11 shows the evolution of compressive strength of the SCC mixture M4, in which 10% LSP and 10% SF were used as mineral fillers. As can be seen from Figure 5.11, the ACC specimens achieved around 92% more strength in 7 days of air exposure after 10 hours of ACC. Although, the degree of carbonation in case of this mixture is lesser due to consumption of $Ca(OH)_2$ by silica from LSP and SF, the strength achievement in air exposure is highest amongst all mixtures. This is due to production of higher amount of C-S-H gel due to primary as well as secondary hydrations taking place during 7 days period of air curing. The strength of the burlap-cured specimens is more than that of the ACC specimens; however, the rate of development of strength of burlap specimens is lower than that of the ACC specimens.

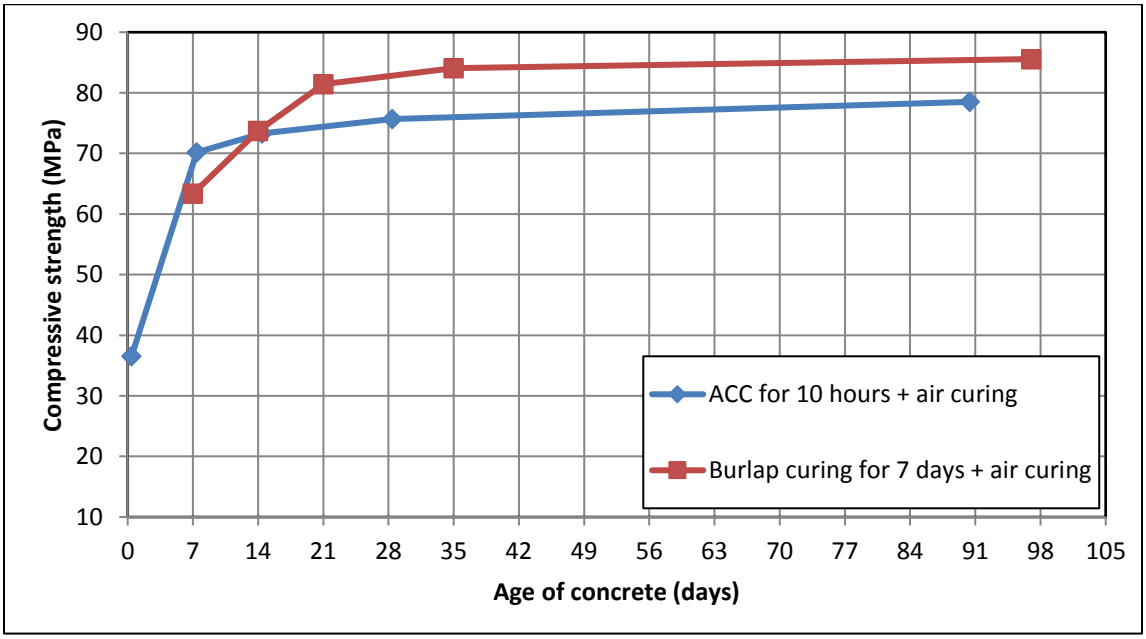

Figure 5.11: Post carbonation effect on compressive strength of M4.

It can be noted from Figure 5.11 that the difference in the strength of ACC and burlap specimens is almost constant (by around 10%) during the long-term air exposure. Therefore, it may be concluded that the difference in the strength of ACC and burlap-cured specimens of mixture M4 will be only 10% during the service life of concrete. Furthermore, the ACC concrete has achieved a strength of 37 MPa only after 10 hours of carbonation making the carbonation-cured concrete able to handle only after 10 hours of curing.

5.5 Splitting tensile strength

Table 5.7 shows the results of splitting tensile strength tests for both ACC and burlap cured specimens belonging to each of the four mixtures. The values of splitting tensile strength, presented in Table 5.7, are plotted in Figure 5.12 to make it more convenient for comparison.

Table 5.7: Split tensile test results for all mixtures.

Mixture ID	Splitting strength (MPa)	
	ACC for 10 hours + 14 days in air	Bur-lapping for 7 days + 7 days in air
M1	3.5	2.9
M2	2.6	3.2
M3	4.0	4.8
M4	5.0	4.6

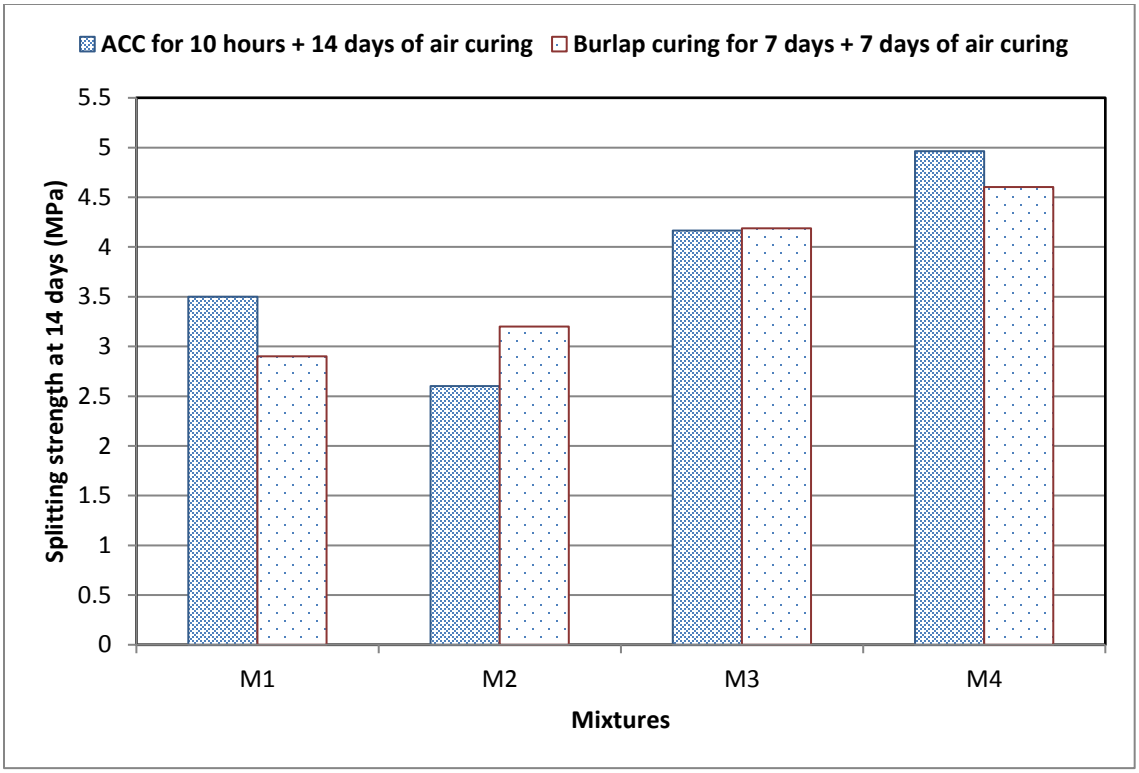

Figure 5.12: Split tensile test results for all mixtures.

As can be seen from Figure 5.12, it is obvious that the ACC improved the tensile strength for the mixtures M1 and M4. For mixtures M1 and M4, the splitting tensile strength was more for ACC specimens than that of burlap specimens by 21% and 8%, respectively. This could be a result of the more exposed surface area to CO_2, which leads to more CO_2 uptake, which in turn creates better dense coat around the specimen leads to higher tensile strength. On the other hand, a slightly decrease in tensile strength of ACC specimens, as compared to burlap specimens, was noticed for mixture M2. No significant difference in the splitting tensile strength of ACC specimens and burlap specimens was noted for the mixture M3. It can be concluded that at the age of 14 days, the performance of ACC specimens is comparable with burlap specimens.

A good correlation exists between the split tensile strength and the compressive strength of the four mixtures, as shown in Figure 5.13.

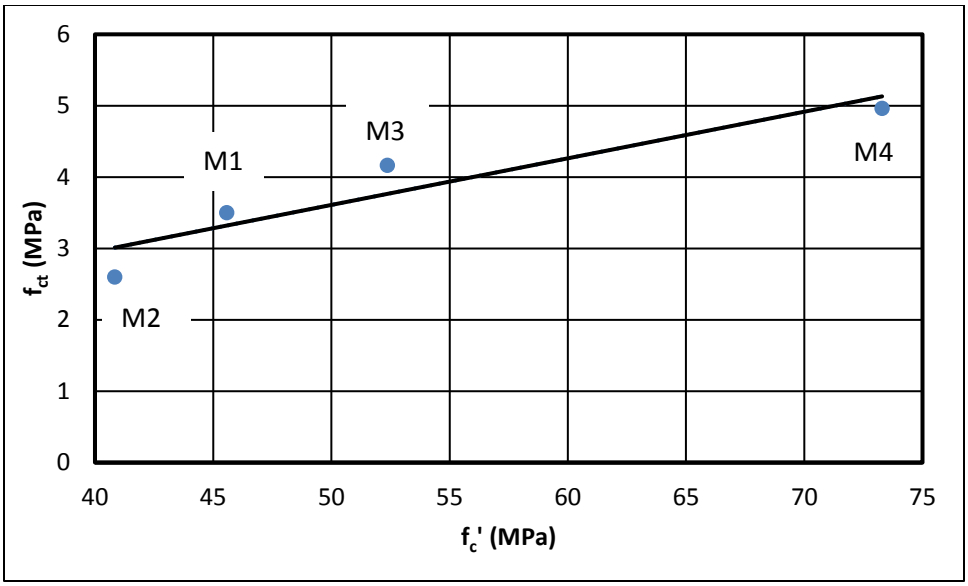

Figure 5.13: Splitting tensile strength versus compressive strength for all mixtures.

5.6 Elastic Modulus

Table 5.8 shows the results of elastic modulus for all four mixtures, tested at the age of 14-days. As mentioned in Table 5.8, before conducting the elastic modulus test, ACC specimens were exposed to air for 14 days after 10 hours of ACC and the burlap specimens were burlap-cured for 7 days and then exposed to air for next 7 days.

Table 5.8: Elastic modulus test results for all mixtures.

Mixture ID	Elastic modulus (GPa)	
	ACC for 10 hours + 14 days in air	Bur-lapping for 7 days + 7 days in air
M1	25.05	26.15
M2	22.20	24.20
M3	33.59	37.76
M4	37.25	36.64

The plot of the values of elastic modulus, as shown in Figure 5.14, indicates that ACC and burlap specimens have approximately the same elastic modulus in both mixtures M1 and M4. For mixtures M2 and M3, ACC specimens show slightly lower values of elastic modulus than that of burlap specimens. However, it can be concluded that the elastic

modulus of ACC specimens at the age of 14 days are comparable with that of the burlap curing.

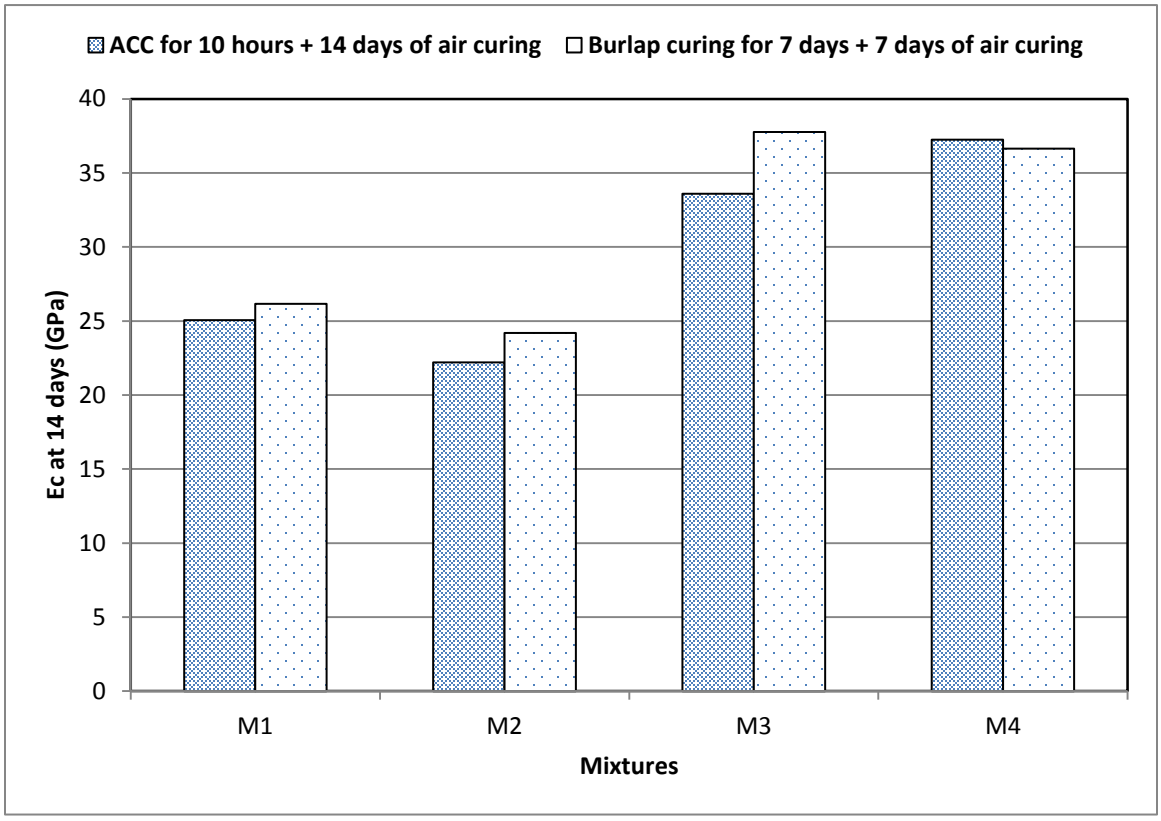

Figure 5.14: Elastic modulus test results for all mixtures.

5.7 Water permeability

The water permeability of concrete is considered as one of the important indicators of the durability of concrete. Based on the water penetration depth measured experimentally, concrete permeability can be classified into three different categories, as shown in Table 5.9 [37].

Table 5.9: Water permeability classification [37].

Water penetration depth range (mm)	Permeability category
$d < 30$	Low
$30 \leq d \leq 60$	Moderate
$d > 60$	High

Table 5.10 shows the results of water penetration depth measured for all four mixtures, at the age of 14-days. Before conducting the water penetration depth test, ACC specimens were exposed to air for 14 days after 10 hours of ACC and the burlap specimens were burlap-cured for 7 days and then exposed to air for next 7 days.

Table 5.10: Water penetration depth for all mixtures

Mixture ID	Water penetration depth (mm)	
	ACC for 10 hours + 14 days in air	Bur-lapping for 7 days + 7 days in air
M1	47.33	52.78
M2	55.33	46.78
M3	20.06	18.83
M4	5.22	6.17

The values of the water penetration depth, as presented in Table 5.10, were plotted as shown in Figure 5.15.

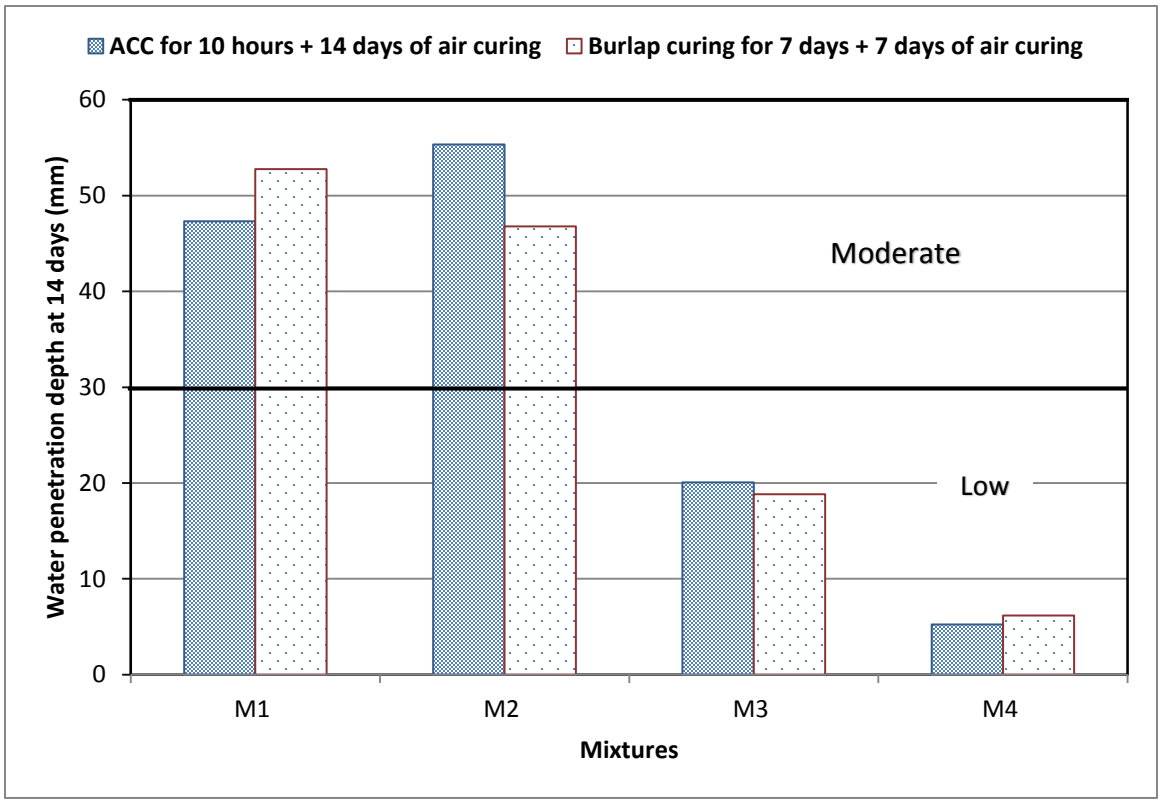

Figure 5.15: Water penetration depth for all mixtures.

It can be observed from Figure 5.15 that while the mixtures M1 and M2 have "moderate" permeability, the mixtures M3 and M4 have "low" permeability. This is because of the use of lower water/binder ratio and higher cementitious materials content (0.30 and 500 kg/m^3, respectively) in cases of the mixtures M3 and M4 as compared to the cases of the mixtures M1 and M2 (0.45 and 375 kg/m^3) [38].

Further, it can be observed from Figure 5.15 that the ACC specimens of mixture M1 showed a lower water penetration depth than that of the burlap specimens. This confirms the fact that the carbonation of concrete makes the microstructure of concrete denser decreasing the porosity of surface concrete that resists the penetration through surface [39]. A higher water penetration of ACC specimens than that of burlap specimens for the mixture M2 is because of a lower degree of carbonation of mixture M2 as it had fly ash replacing Portland cement partially by 20%. Because of 20% lower Portland cement content as compared with the mixture M1, the rate of the formation of $CaCO_3$-C-S-H layer around the concrete specimens was slow down which in turn led to lower densification in case of the mixture M2.

In case of mixtures M3 and M4, the water penetration depths for ACC specimens and burlap specimens are almost same. The positive effect of carbonation is not visible in case of mixtures M3 and M4 because of the major densification effect of lower water/binder ratio and higher cementitious materials content used in mixtures M3 and M4.

It can be concluded that the water permeability of ACC specimens at the age of 14 days are comparable with that of the burlap curing.

5.8 Chloride permeability

Rapid Chloride Penetration Test (RCPT) is the most commonly method used to measure chloride permeability [40]. ASTM C 1202 provides the procedures for this test [31]. Although RCPT method is not perfect for all types of concrete mixtures, especially for concretes with cementitious materials or chemical admixtures, this method is still the simplest and the fastest [41]. Based on the measured values of charges passing through

concrete, the chloride permeability can be classified into five different categories, as presented in Table 5.11.

Table 5.11: Different chloride permeability categories [41].

Chloride permeability	Charge passing (Coulombs)	Typical concrete type
High	> 4000	High w-c ratio (> 0.6) conventional PC concrete.
Moderate	2000 to 4000	Moderate w-c ratio (0.40 to 0.50) conventional PC concrete.
Low	1000 to 2000	Low w-c ratio (< 0.40) conventional PC concrete.
Very low	100 to 1000	Latex-modified concrete, internally sealed concrete.
Negligible	< 100	Polymer-impregnated concrete, polymer concrete.

The results of chloride permeability measured for all four mixtures, at the age of 14-days, are presented in Table 5.12. Figure 5.16 shows the plots of chloride permeability values. It can be observed from Figure 5.16 that the mixtures M1 and M2 have "moderate" chloride permeability, the mixture M3 has "low" chloride permeability, and mixture M4 has "very low" permeability. This is because of the use of lower water/binder ratio and higher cementitious materials content in cases of the mixtures M3 and M4 as compared to the cases of the mixtures M1 and M2.

Table 5.12: Chloride penetration results for all mixtures.

Mixture ID	Chloride permeability (Coulombs)	
	ACC for 10 hours + 14 days in air	Bur-lapping for 7 days + 7 days in air
M1	2960	3439
M2	3844	3282
M3	1099	1246
M4	244	285

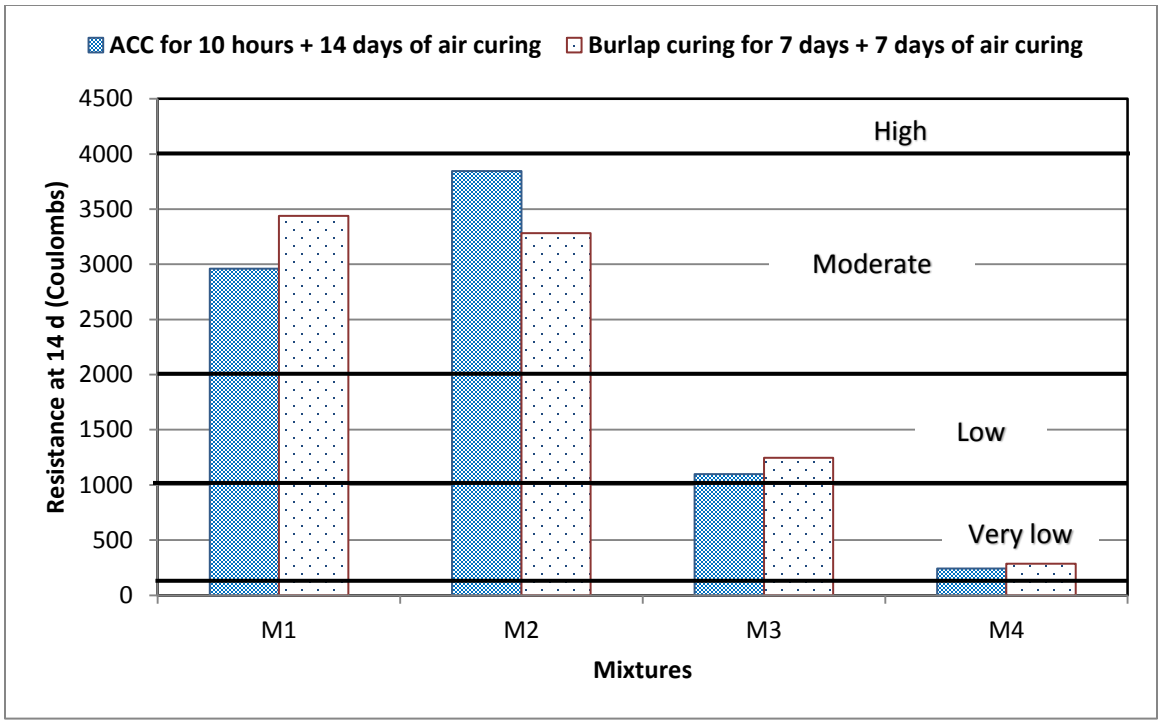

Figure 5.16: Chloride penetration results for all mixtures.

It can be observed from Figure 5.16 that the ACC specimens of mixture M1 showed a lower chloride permeability than that of the burlap specimens because of the beneficial effect of carbonation in achieving a denser microstructure of surface concrete, as mentioned in the previous section. A higher chloride permeability of ACC specimens than that of burlap specimens for the mixture M2 is because of a lower degree of carbonation of mixture M2 as it had fly ash replacing Portland cement partially by 20% leading to lower densification in case of the mixture M2, as described in the previous section.

In case of mixtures M3 and M4, the chloride permeability for ACC specimens and burlap specimens are almost same. The reason for this is same as mentioned in the previous section on water permeability.

It can be concluded that the chloride permeability of ACC specimens at the age of 14 days are comparable with that of the burlap curing.

5.9 Drying shrinkage

Monitoring of shrinkage of both ACC specimens as well as burlap specimens started directly after curing (10 hours for ACC and 7 days for burlap) and lasted up to 180 days. The shrinkage at the early age was recorded more frequently than at the later age because of the fact that the shrinkage in the beginning takes place rapidly. Figures 5.17 through 5.20 show the variations of drying shrinkage with time for ACC and burlap specimens belonging to the mixtures M1, M2, M3 and M4, respectively.

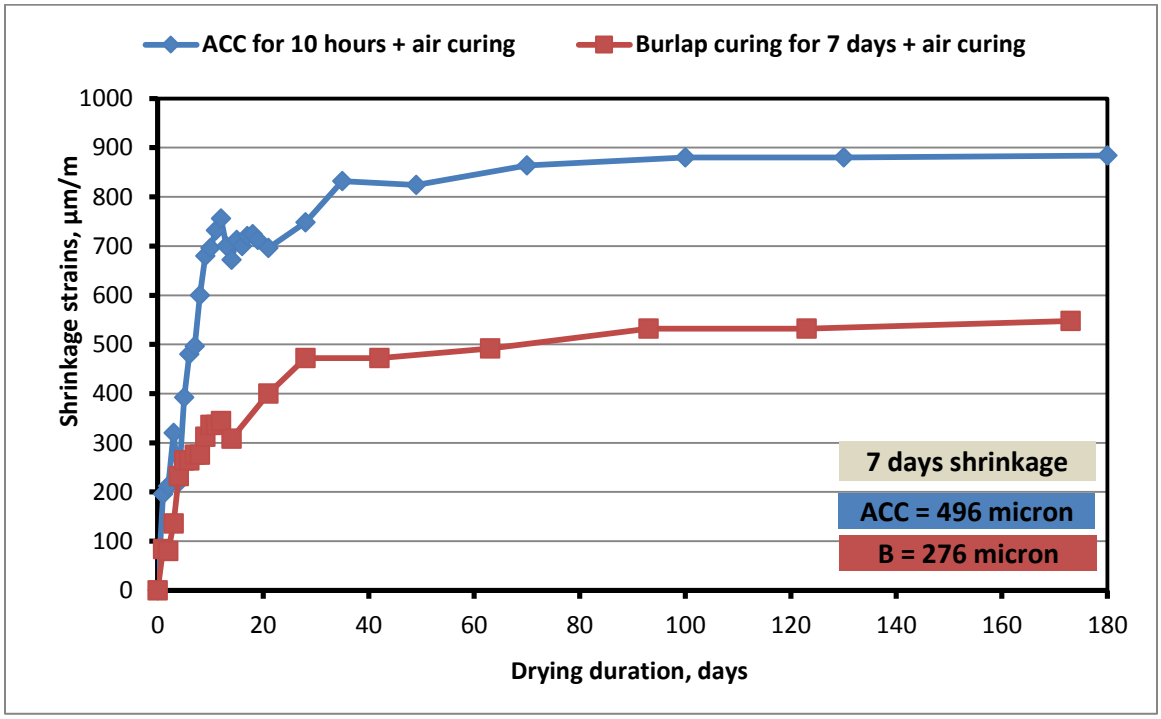

Figure 5.17: Drying shrinkage strain-time plot for M1.

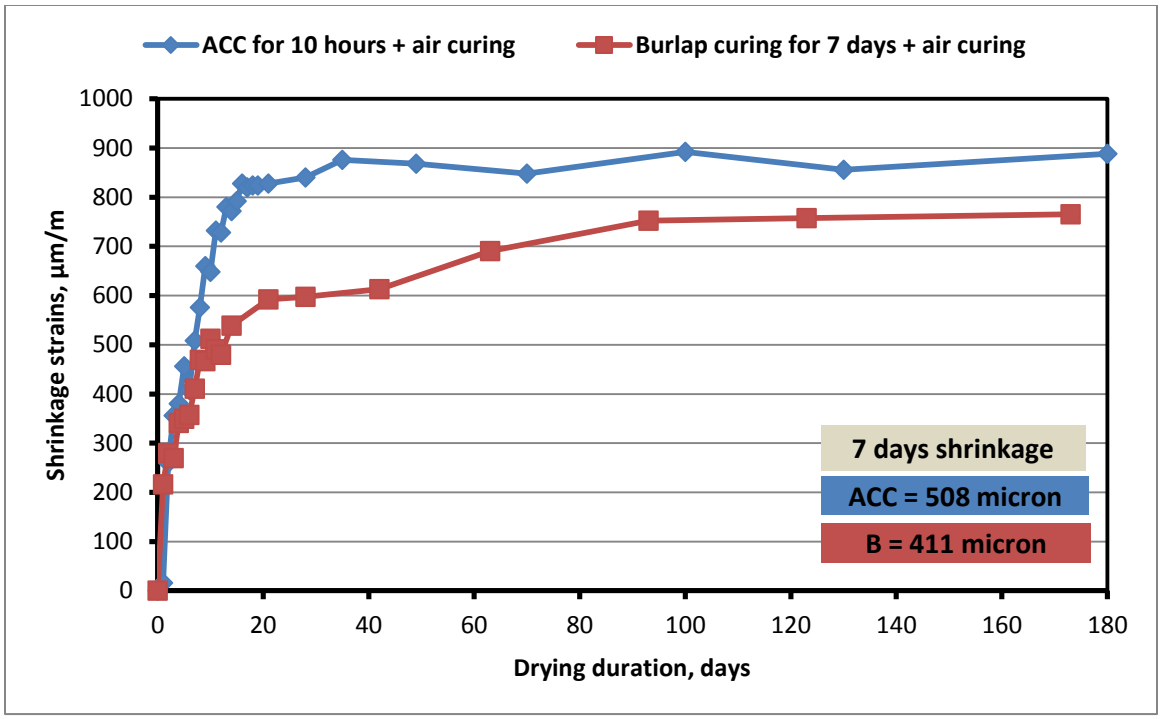

Figure 5.18: Drying shrinkage strain-time plot for M2.

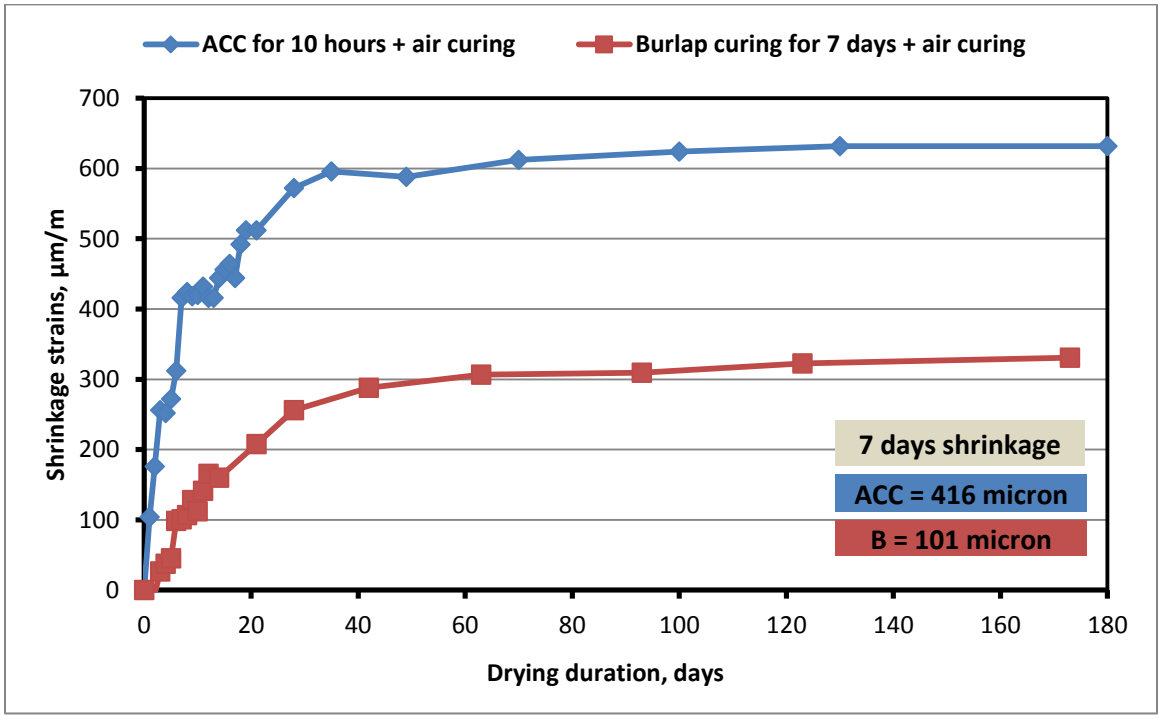

Figure 5.19: Drying shrinkage strain-time plot for M3.

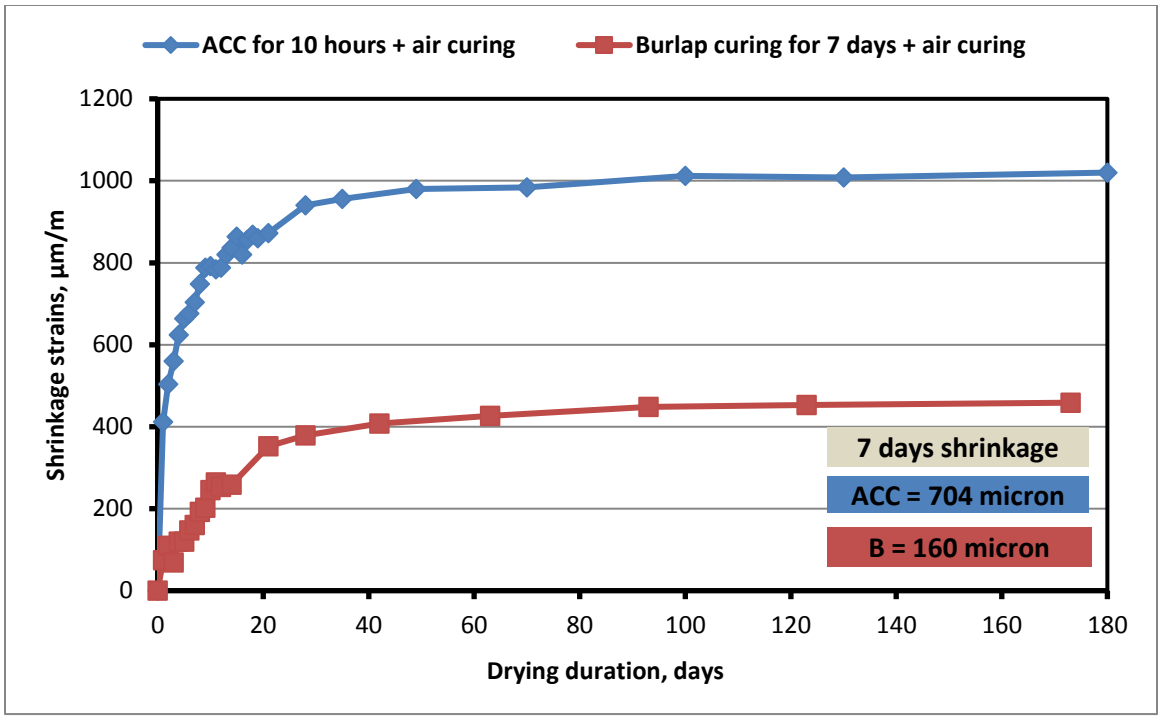

Figure 5.20: Drying shrinkage strain-time plot for M4.

For all four mixtures, the shrinkage in ACC specimens was more than that of burlap-cured specimens as evident from Figures 5.17 through 5.20. Higher shrinkage in ACC specimens may be attributed to the shrinking action associated with the chemical reactions involved in carbonation of the surface concrete. However, as noted from Figures 5.17 through 5.20, the 7 days shrinkage of ACC specimens for all the mixtures is either less than or almost same as the maximum limit of 500 microns except that of mixture M4. Very high shrinkage in the ACC specimens made of mixture M4 is because the ultrafine particles of SF increased the surface area of binders, which led to a faster hydration and water consumption at the surface of the specimens. However, this problem of high shrinkage in ACC specimens of the mixture M4 expected to be solved by spraying water on the surface of the specimens directly after the ACC.

Overall, ACC specimens show an acceptable shrinkage strain far all mixtures except M4 that can be reduced by supplying water to the specimens directly after ACC to compensate the water loss due to faster hydration caused by ultrafine particles of silica fume on the surface.

5.10 Concrete characterization

This section discusses scanning electron microscopy (SEM), Energy-dispersive X-ray spectroscopy (EDS) and X-ray Diffraction (XRD) of all mixtures cured with ACC regime. Concrete samples for each mixture were tested after ACC.

5.10.1 SEM, EDS and XRD for M1

Figure 5.21 shows a micrograph of a fractured specimen exposed to optimal ACC. The lower edge of the image represents the surface edge of the concrete fracture, the red line is the actual profile of the carbonated area penetrated by CO_2, and the double arrow line indicates the average of the actual profile.

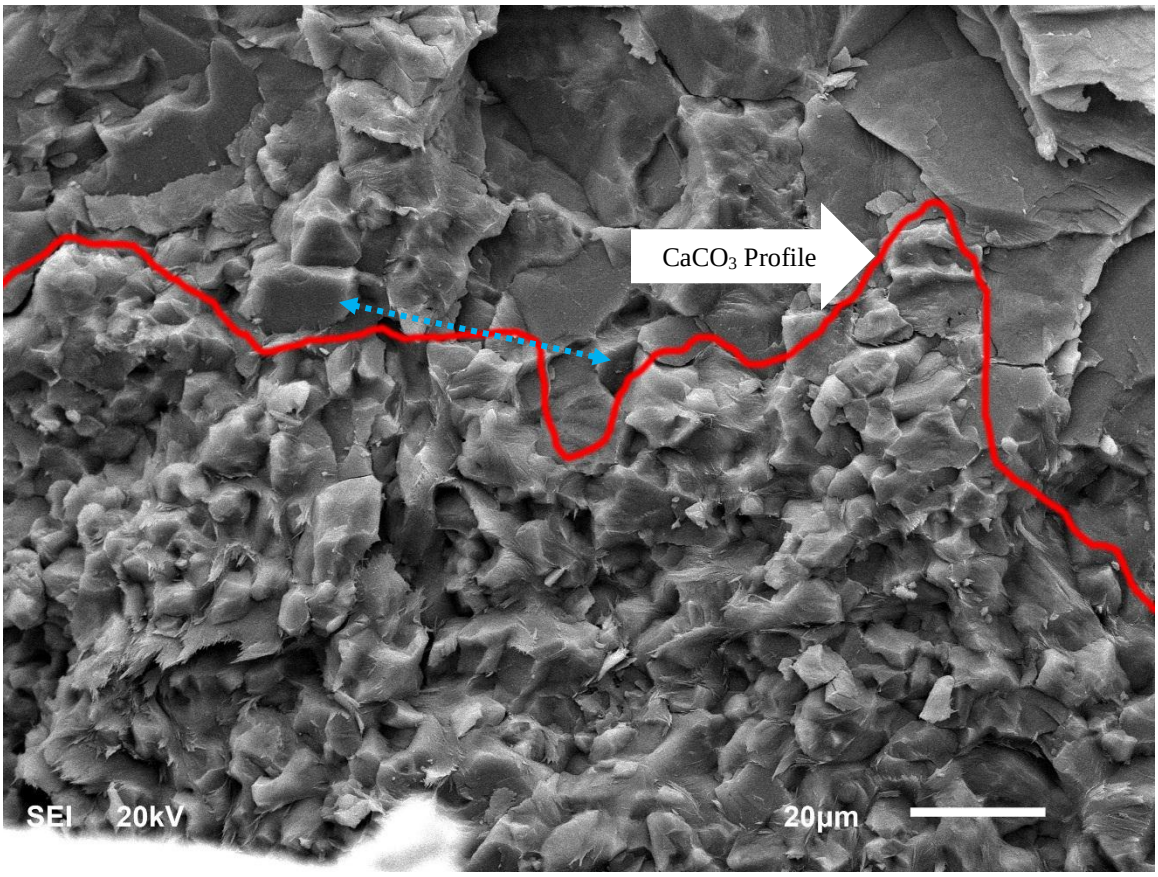

Figure 5.21: SEM micrograph of M1.

The dense structure of hydrates shown in Figure 5.21 is due to the formation of $CaCO_3$, formed by the accelerated carbonation of Portlandite, $Ca(OH)_2$, and conventional calcium silicate hydrate (C-S-H). The intermixing between $CaCO_3$ and C-S-H may be explained by

the fact that the primary C-S-H was highly porous after about 18 hours of casting, when the ACC was commenced. Subsequently, the pores were available for diffusion of CO_2 and conversion of the Portlandite formed resulting in the formation of $CaCO_3$. Based on the scale of SEM image, the carbonation depth is estimated as 80 microns, which is correlated with what was found previously using phenolphthalein spray (Section 5.3).

Improving microstructure and formation of the protective dense layer can be seen clearly in Figure 5.22, which was taken from Figure 5.21 as spectrum 8. Obviously, ACC reduce the permeability significantly by filling the pores and minor cracks with $CaCO_3$. Furthermore, this layer may reduce the evaporation of the internal water in the long run and this means that the concrete will have self-curing. All this explains the improved properties of the concrete cured with ACC method.

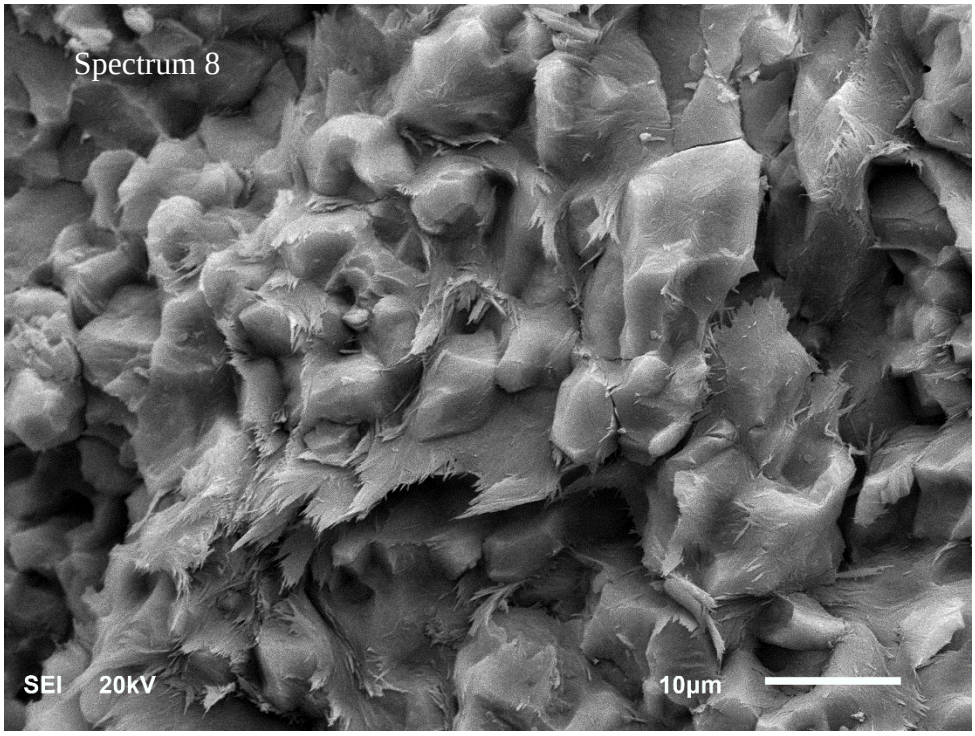

Figure 5.22: Close view in the carbonared area of M1.

Beside the SEM images, EDS was also conducted to figure out the chemical composition of the cured sample. Figure 5.23 show the EDS profile of spectrum 8.

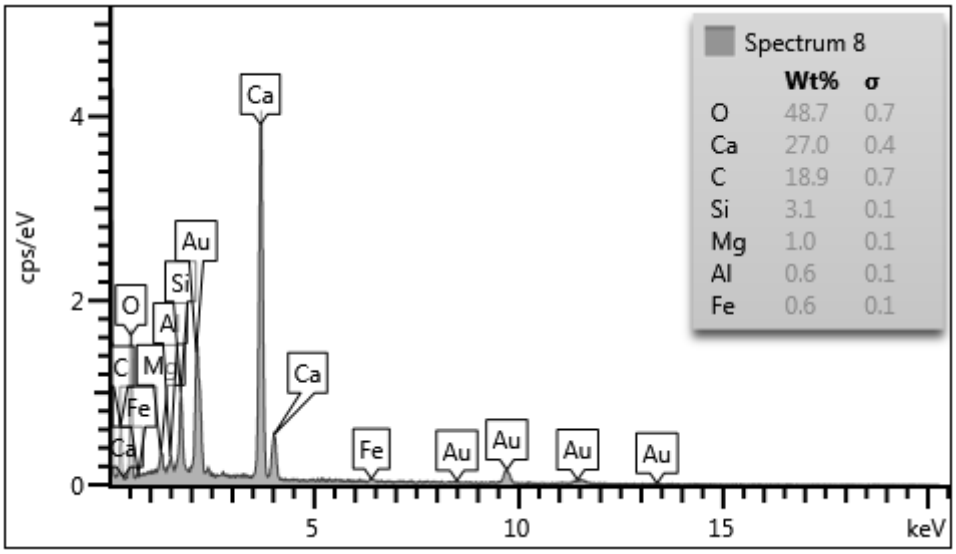

Figure 5.23: EDS of M1.

The EDS indicates a high carbon content of 18.9% and low amount of silica 3.1%, showing that the area probably contains a significant amount of $CaCO_3$ along with C-S-H.

Figures 5.24 and 5.25 depict the mineralogical composition of concrete specimens cured with ACC as well as burlap method. Formation of quartz (contributed by sand), calcite and Portlandite is noted in both the specimens. However, the quantity of Portlandite in ACC specimen is less than that of burlap because of consuming of $Ca(OH)_2$ due to ACC.

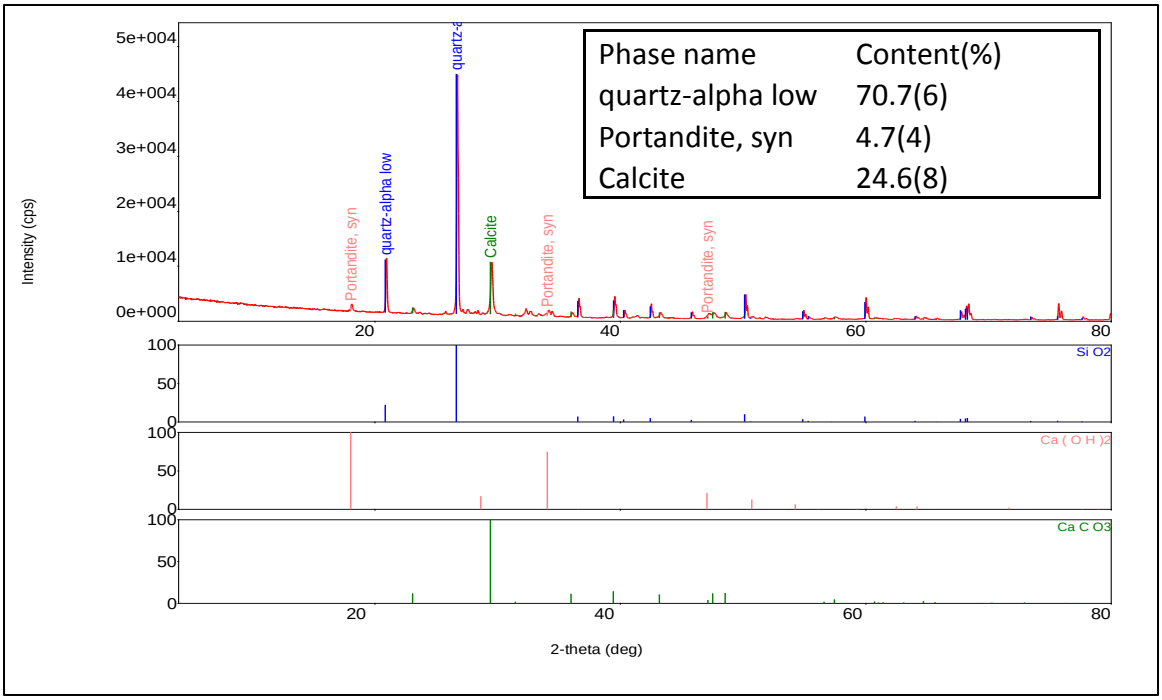

Figure 5.24: XRD of M1.

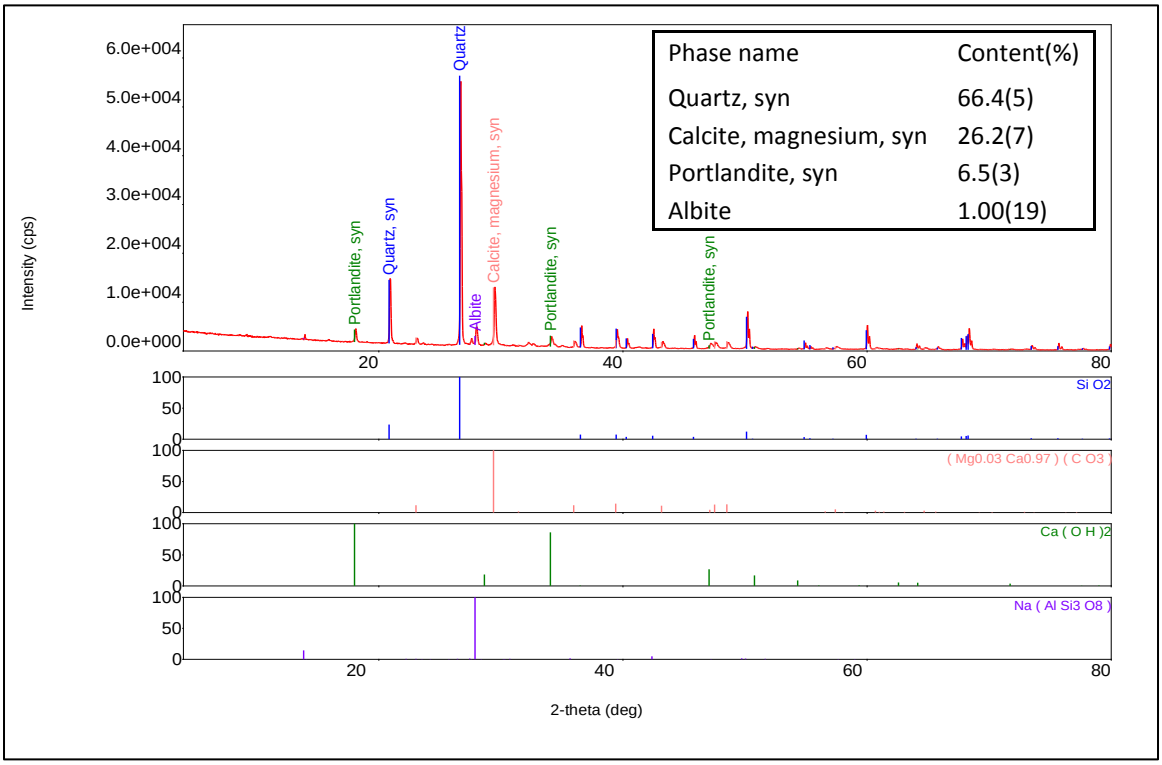

Figure 5.25: XRD of M1 (burlap specimen).

5.10.2 SEM, EDS and XRD for M2

Figure 5.26 shows a micrograph of a fractured specimen exposed to optimal ACC. There was some carbonation can be recognized but the amount of produced $CaCO_3$ was less than that of M1 and this is because of the lower cement content.

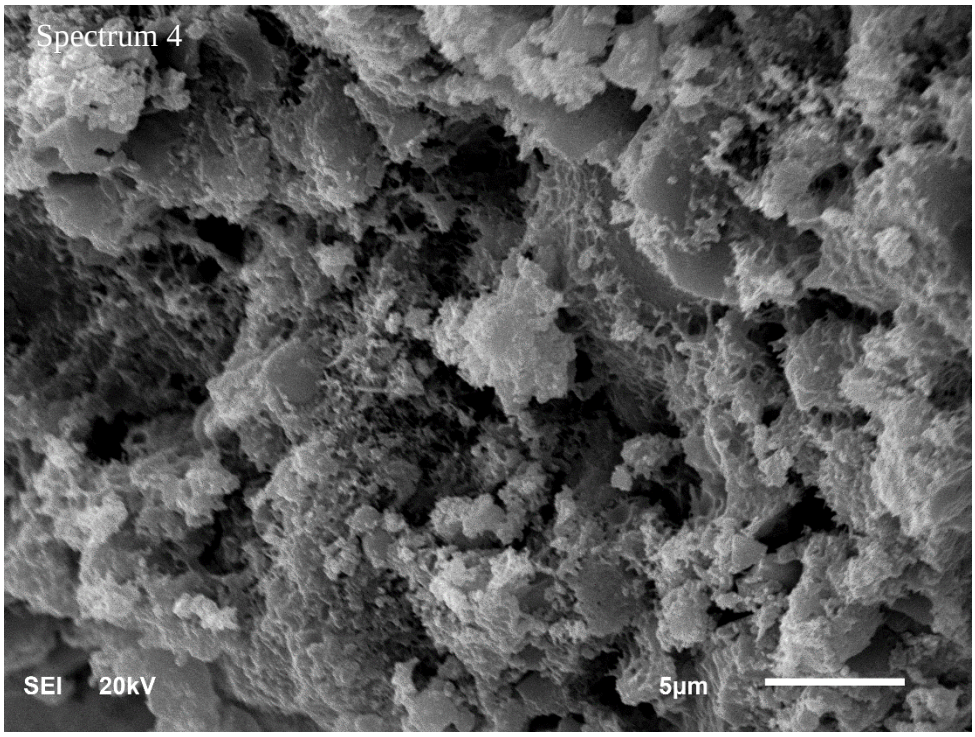

Figure 5.26: SEM micrograph of M2.

Figure 5.27 shows the EDS of the area represented by spectrum 4. This emphasizes the fact that M2 gained lower degree of carbonation than M1 since the amount of silica is considered a little bit higher (8.7%) when it was only (3.1%) in M1 case. Further, XRD show that the calcite content dropped from 24.6% in M1 to 15.2% in the mixture M2 (Figure 5.28). It seems that 20% replacement of fly ash affects the degree of carbonation negatively. All this may explain why ACC specimens of M2 exhibited lower improving in comparison with M1 in properties discussed earlier such as water permeability and chloride permeability.

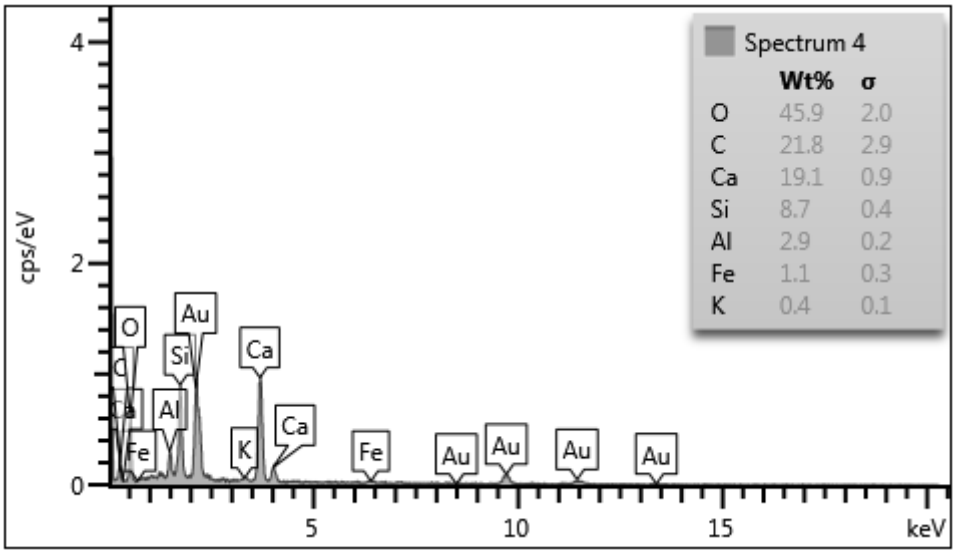

Figure 5.27: EDS of M2.

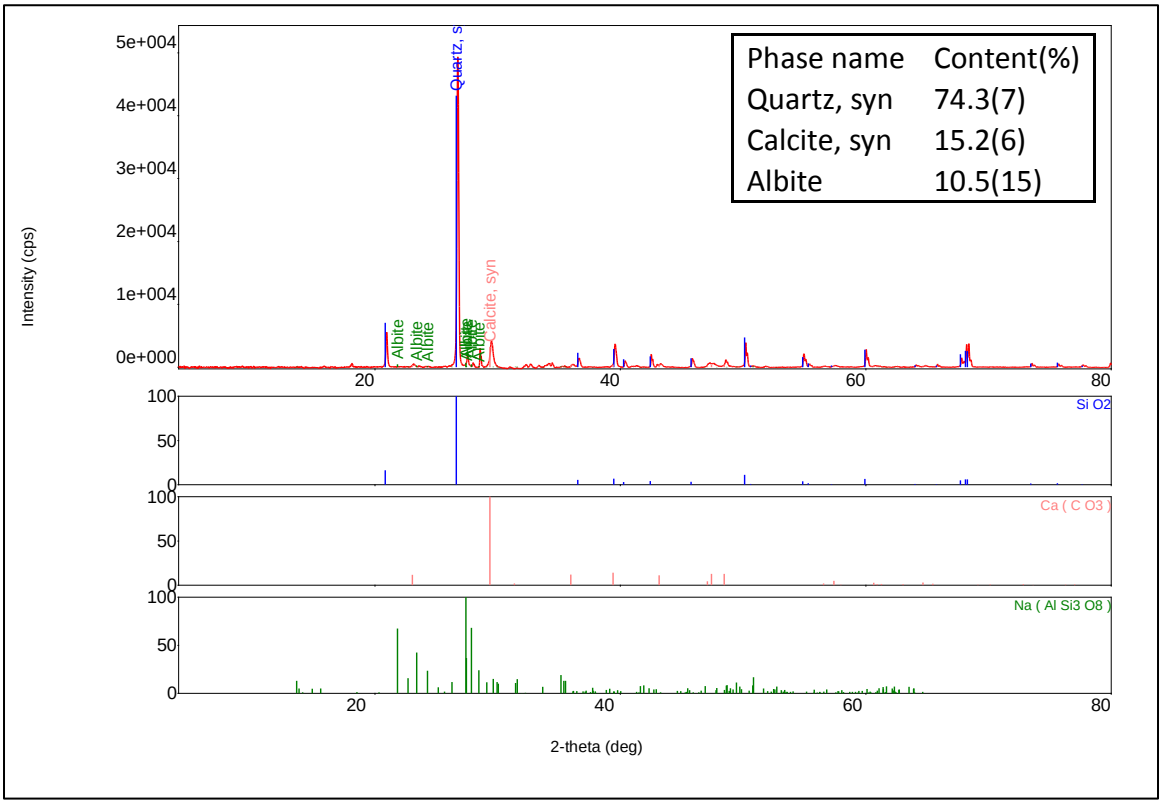

Figure 5.28: XRD of M2.

5.10.3 SEM, EDS and XRD for M3

The SCC M3 with 20% LSP of the total cementitious materials was exposed to optimal ACC. Figure 5.29 shows SEM of concrete portion taken from specimen surface. The left edge of the figure represents the concrete surface.

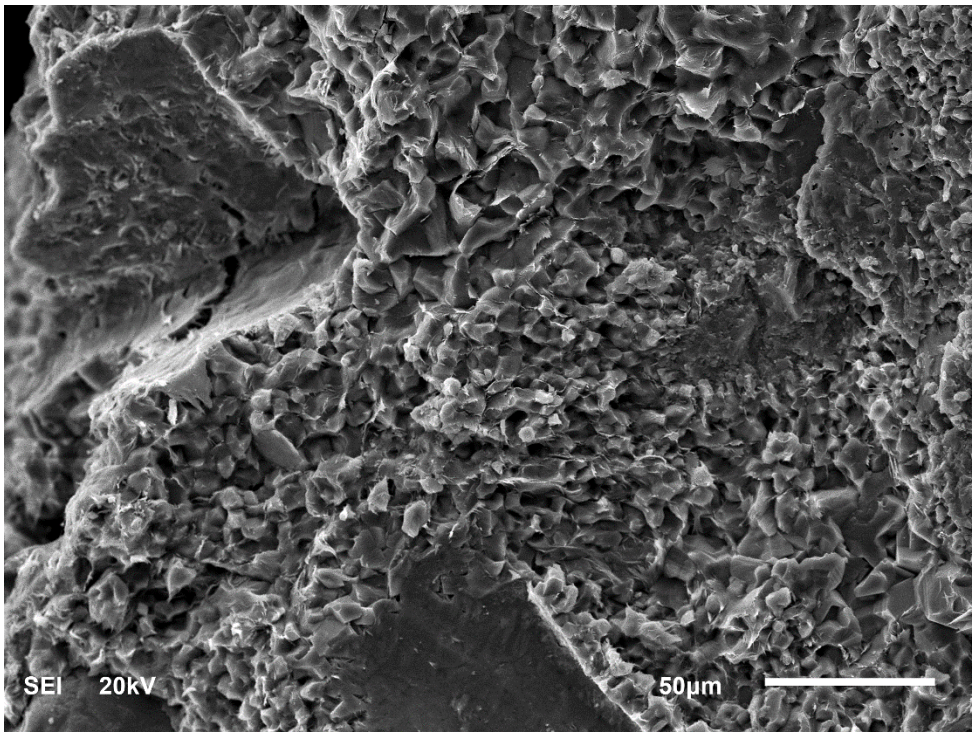

Figure 5.29: SEM micrograph of M3.

It is obvious from Figure 5.29 that $CaCO_3$ forms at the edges of the cured specimen. This change in the microstructure can be recognized in a better way in Figure 5.30 with higher magnification. The formed calcite block the fine pores structure and increase the density of the carbonated area of the concrete specimen.

Figure 5.32 shows the EDS of the whole area represented by spectrum 3 in Figure 5.31. The result pointed out the presence of the high carbon content (16.8%) beside low amount of silica (1.9%). XRD outcomes were illustrated in Figure 5.33 that show 15.8% of calcite was formed in that sample.

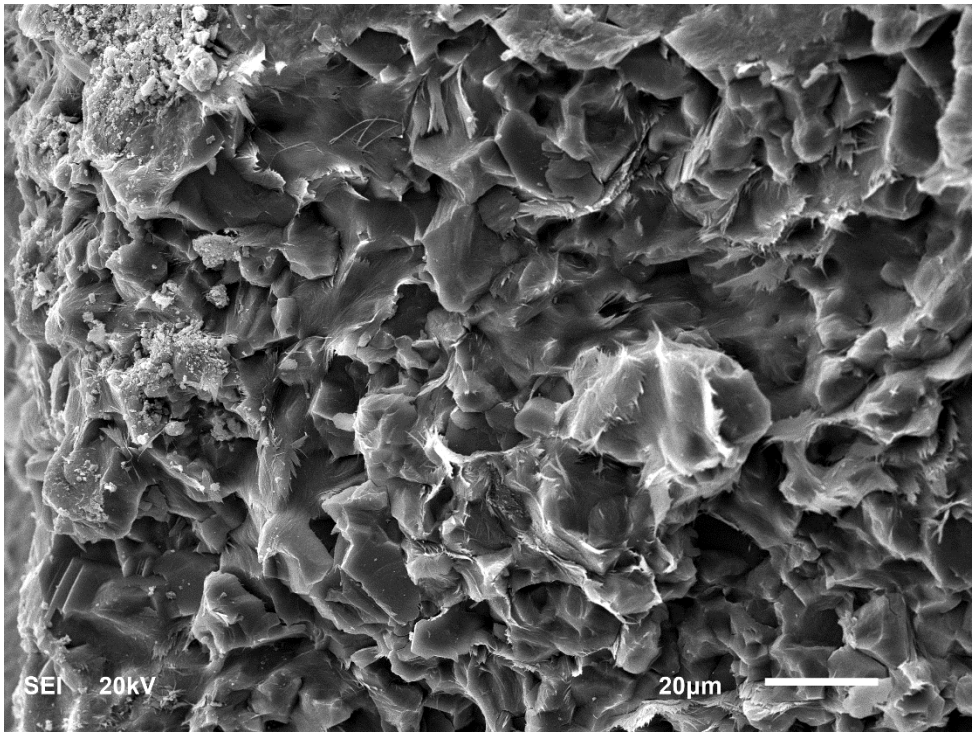

Figure 5.30: Close view in the carbonared area of M3.

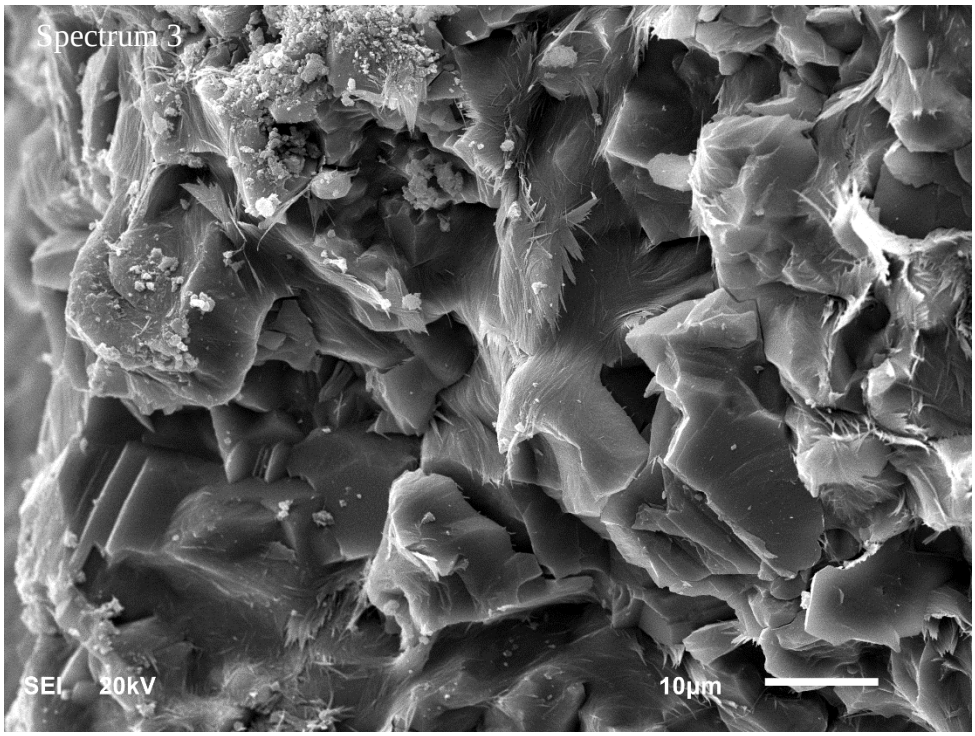

Figure 5.31: Spectrum 3 of M3.

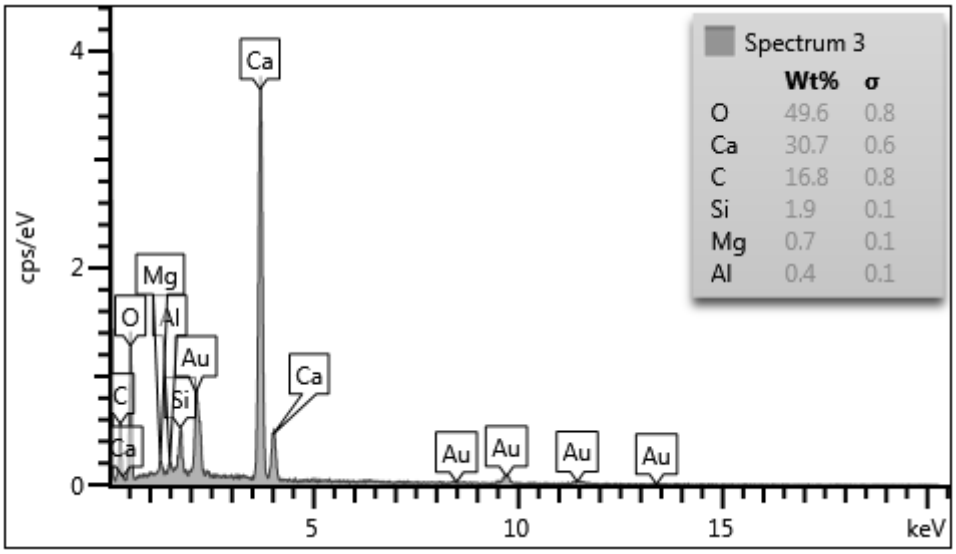

Figure 5.32: EDS of M3.

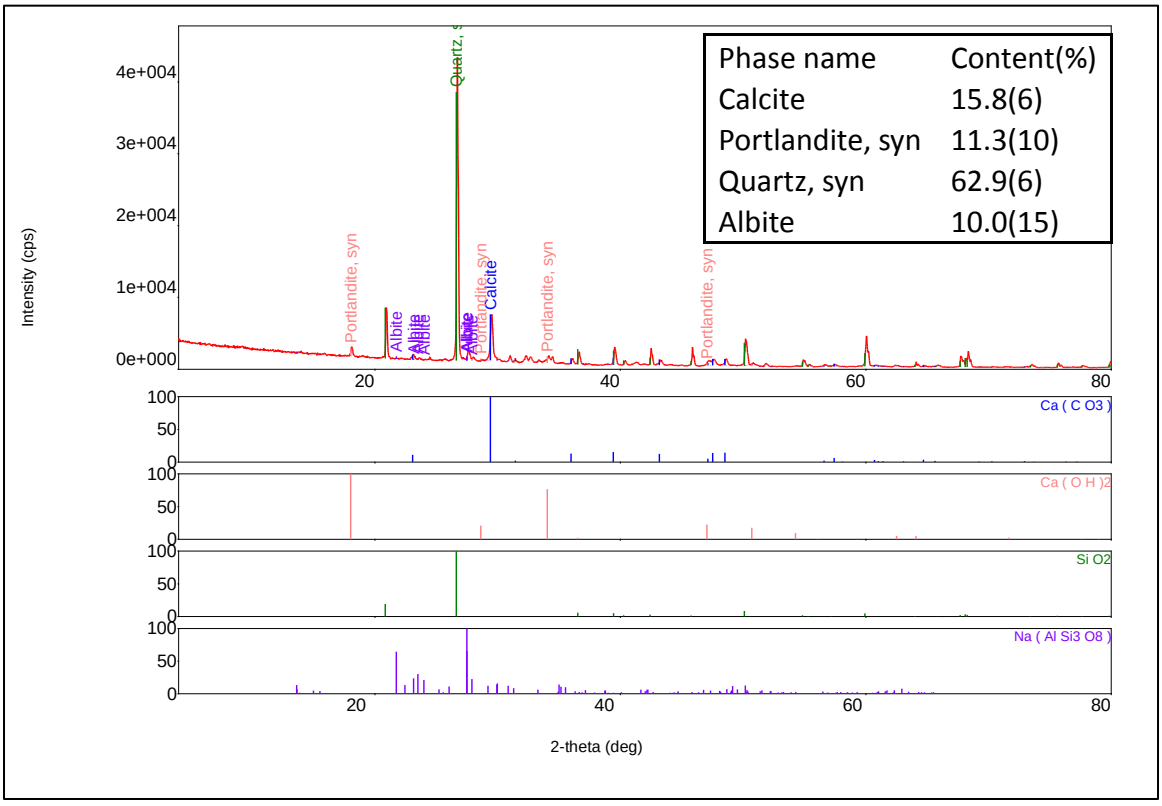

Figure 5.33: XRD of M3.

5.10.4 SEM, EDS and XRD for M4

Figure 5.34 shows a micrograph of a fractured specimen of the SCC mixture M4 with 10% of LSP and 10% of SF from the total cementitious materials exposed to optimal ACC. The left edge of the figure represents the concrete surface.

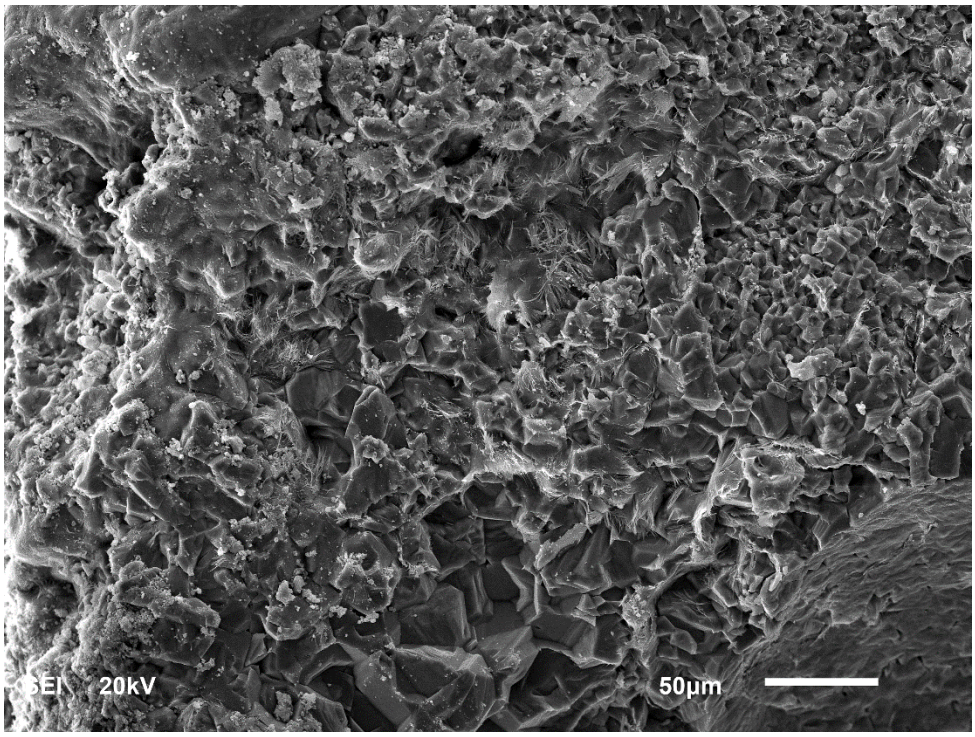

Figure 5.34: SEM micrograph of M4.

The formation of $CaCO_3$ at the edges of the cured specimen is very clear. The densification in the microstructure can be recognized in a better wayin Figure 5.35 with higher magnification. The formed calcite block the fine pores structure and increase the density of the carbonated area of the concrete specimen.

Figure 5.37 presents the EDS of the whole area represented by spectrum 4 in Figure 5.36. The result pointed out the presence of the high carbon content (16.4%) beside low amount of silica (1.2%). XRD outcomes were illustrated in Figure 5.38 that show 21% of calcite was formed in that sample. All this may reflected to the fact that ACC specimens of M4 exhibited significant improving in properties discussed earlier such as water permeability and chloride permeability.

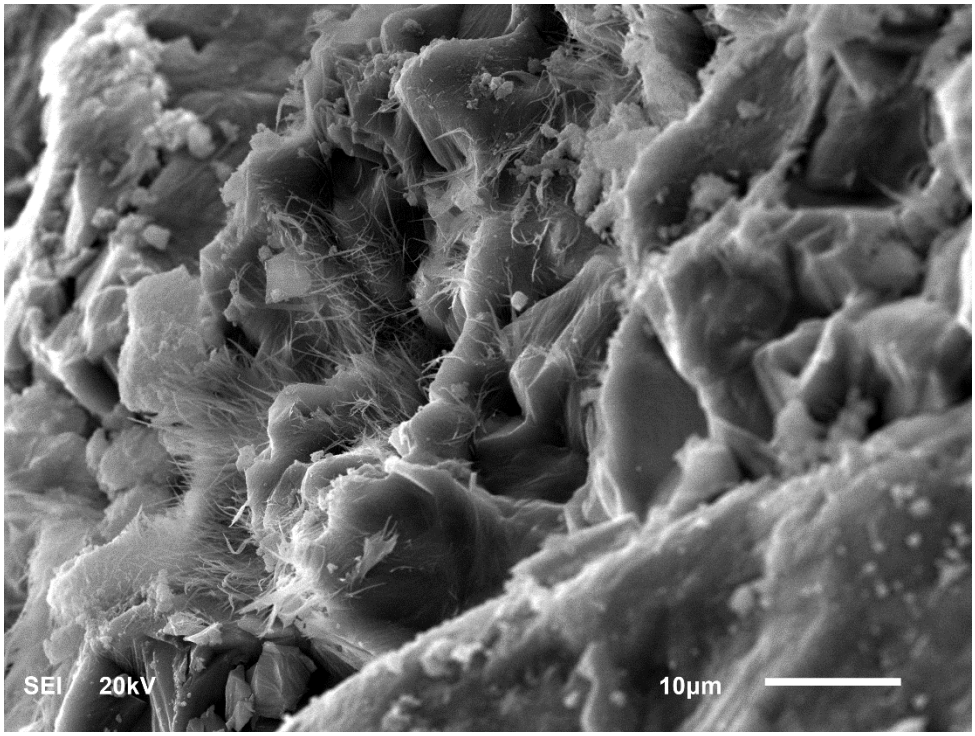

Figure 5.35: Close view in the carbonared area of M4.

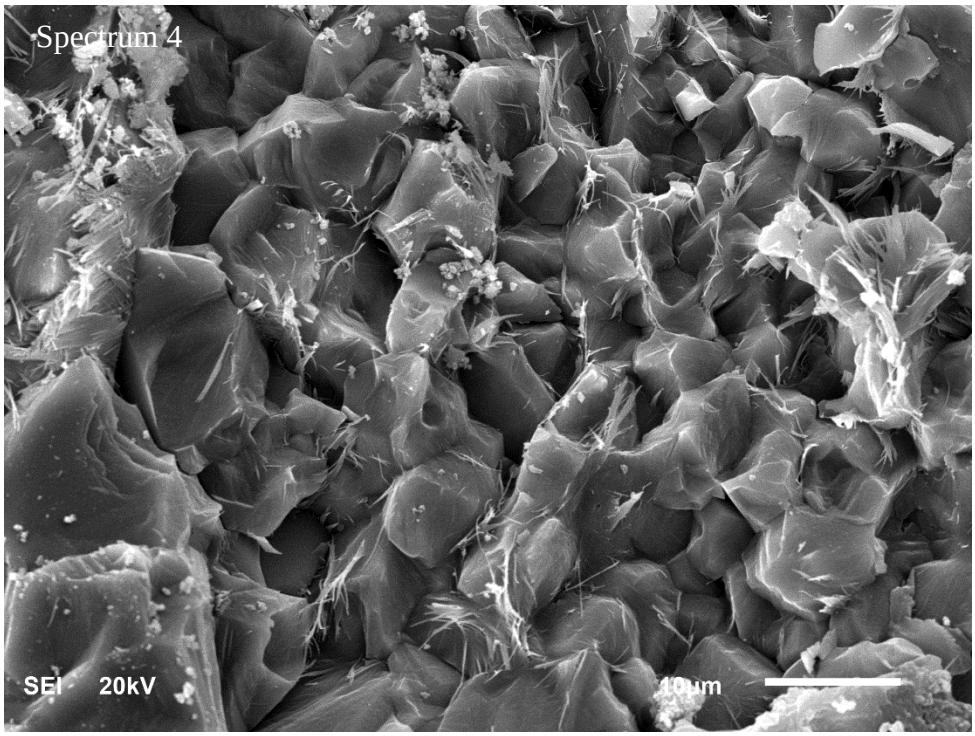

Figure 5.36: Spectrum 4 of M4.

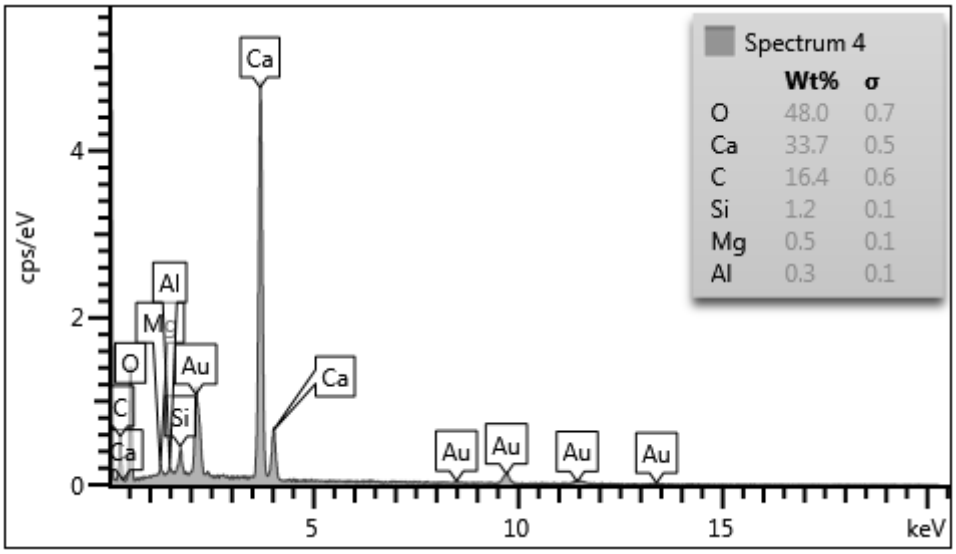

Figure 5.37: EDS of M4.

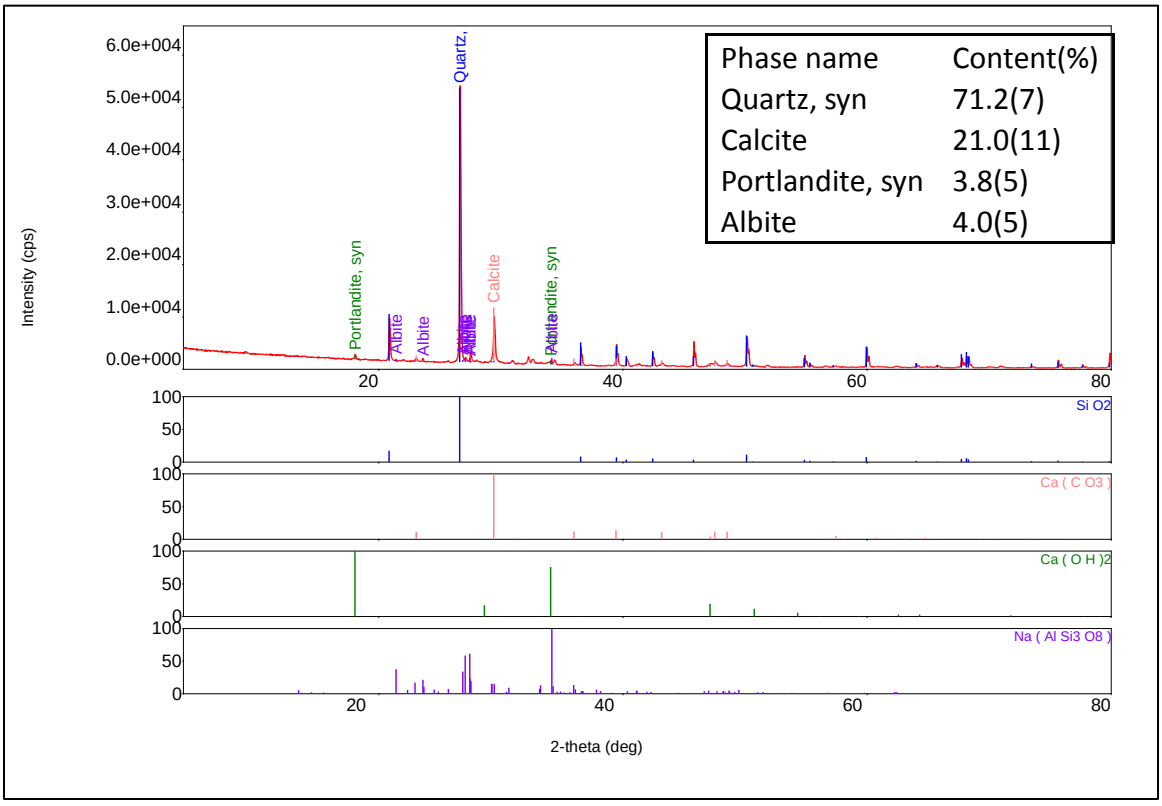

Figure 5.38: XRD of M4.

Overall, the characterization of the ACC specimens illustrate the morphology and minerology changes occur due to ACC and give a logical explanation of other tests results.

CHAPTER 6

CONCLUSIONS AND RECOMMENDATIONS

6.1 Conclusions

Based on the findings of the present study, following conclusions can be drawn:

i. The ACC duration appears to control the evolution rate of strength and weight gain, rather than the ACC pressure. The evolution of compressive strength during the course of ACC is periodically progressive, rather than steadily progressive.

ii. Accelerated carbonation curing (ACC) at an optimal pressure of 60 psi and a duration of 10 hours was found to be most effective.

iii. The carbonation depth did not exceed 2 mm for all mixtures, which is considered as a safe depth for a reinforced concrete with a minimum cover of 20 mm.

iv. The increase in strength due to ACC for 10 hours were found to be 79, 63, 41, and 34%, respectively, for mixtures M1, M3, M4, and M2 depending on the silica from mineral admixture. The mixture M1 had highest strength gain because of the higher degree of carbonation due to availability of higher $Ca(OH)_2$ in the absence of silica as it had no mineral admixture. The decreasing trend of strength gain in case of the mixtures M3, M4, and M2 was according to the increased amount of silica contributed from the mineral admixtures added to them. However, for all the four mixtures, the strength after 10 hours of ACC was more than 20 MPa. Therefore, the concrete components made using all four mixtures can be handled and transported immediately after 10 hours of ACC.

v. The increase in strength after 7 days of air exposure followed by ACC was found to be around 60% for the mixtures M1, M2, and M3. This increase was very high

(92%) in case of the mixture M4 because of the positive effect of silica fume participating in secondary hydration during first 7 days of air exposure.

vi. The difference between strength of ACC and burlap-cured specimens was in the range of 5 to 26%.

vii. Tensile strength, modulus of elasticity, water penetration depth, and chloride permeability of ACC specimens were found to be comparable with that of the burlap specimens.

viii. Although the shrinkage of ACC specimens was higher than that of burlap specimens for all the mixtures, 7 days shrinkage of ACC specimens was less or almost same as permissible shrinkage except for the mixture M4, which can be controlled by spraying water on concrete immediately after ACC.

ix. SEM of the ACC specimens indicated the formation of calcite at the surface while C-S-H was noted in the un-carbonated area. In the intermediate areas, the presence of both calcite and C-S-H was noted. XRD also indicates the formation of these two minerals.

6.2 Recommendations from this work

1. Depending on the required compressive strength, optimization curve (Figure 5.1) could be used to determine the appropriate pressure and duration of ACC.

2. ACC method is recommended for curing the precast concrete elements due to the following advantages of ACC, revealed through the present work:

    a. The strength of mixtures immediately after 10 hours of ACC was more than 20 MPa (so that the concrete products can be handled and transported quickly);

    b. A very small difference in strengths of ACC and burlap-cured specimens during service life;

c. Other mechanical and durability properties of ACC specimens comparable with burlap specimens;

d. Acceptable shrinkage of ACC specimens

e. No effect of carbonation on reinforcement corrosion due to a very shallow depth of carbonation

6.3 Recommendations for future work

1. The possibility to reduce the initial air curing prior to ACC, should be investigated to reduce the gross curing time.
2. Other durability properties, such as corrosion potential, corrosion current density and sulfate resistance, should be investigated to assess such a curing regime very well.
3. The effect of ACC on other concretes, such as lightweight concrete and UHPC have to studied as these types of concrete may open new avenue for ACC process.

REFERENCES

[1] V. Rostami, Y. Shao, A. J. Boyd, and Z. He, "Microstructure of cement paste subject to early carbonation curing," Cement and Concrete Research, vol. 42, no. 1, pp. 186–193, 2012.

[2] M. Fernandez Bertos, S. J. Simons, C. D. Hills, and P. J. Carey, "A review of accelerated carbonation technology in the treatment of cement-based materials and sequestration of CO_2," J Hazard Mater, vol. 112, no. 3, pp. 193–205, 2004.

[3] Y. Shao, "Carbonation curing of slag-cement concrete for binding CO_2 and improving performance," Journal of Materials in Civil Engineering, vol. 22, no. 4, pp. 296-304. 2010.

[4] J. Jerga, "Physico-mechanical properties of carbonated concrete," Construction and Building Materials, vol. 18, no. 9, pp. 645–652, 2004.

[5] B. Zhan, C. S. Poon, Q. Liu, S. Kou, and C. Shi, "Experimental study on CO_2 curing for enhancement of recycled aggregate properties," Construction and Building Materials, vol. 67, pp. 3-7, 2013.

[6] S. Monkman and Y. Shao, "Integration of carbon sequestration into curing process of precast concrete," Canadian Journal of Civil Engineering, vol. 37, no. 2, pp. 302–310, 2010.

[7] S. Kashef-Haghighi and S. Ghoshal, "Physico–chemical processes limiting CO_2 uptake in concrete during accelerated carbonation curing," Industrial & Engineering Chemistry Research, vol. 52, no. 16, pp. 5529–5537, 2013.

[8] S. Monkman and R. Niven, "Integration of carbon dioxide curing into precast concrete production," Carbon Sense Solutions, Canada, 2010, pp. 1–9, 2010.

[9] L. Mo and D. K. Panesar, “Accelerated carbonation – A potential approach to sequester CO_2 in cement paste containing slag and reactive MgO,” Cement and Concrete Composites, vol. 43, pp. 69–77, 2013.

[10] Y. Shao and S. Monkman, “A new CO_2 sequestration process via concrete products production,” IEEE EIC Climate Change Conference, 2006.

[11] V. Rostami, Y. Shao, and A. J. Boyd, “Durability of concrete pipes subjected to combined steam and carbonation curing,” Construction and Building Materials, vol. 25, no. 8, pp. 3345–3355, 2011.

[12] Y. Shao, V. Rostami, Z. He, and A. J. Boyd, “Accelerated carbonation of portland limestone cement,” Journal of Materials in Civil Engineering, vol. 26, no. 1, pp. 117–124, 2014.

[13] Y. Shao, M. S. Mirza, and X. Wu, “CO_2 sequestration using calcium-silicate concrete,” Canadian Journal of Civil Engineering, vol. 33, no. 6, pp. 776–784, 2006.

[14] M. K. Mohammed, A. R. Dawson, and N. H. Thom, “Carbonation of filler typed self-compacting concrete and its impact on the microstructure by utilization of 100% CO_2 accelerating techniques,” Construction and Building Materials, vol. 50, pp. 508–516, 2014.

[15] D. P. Chen, J. Y. Liu, M. Liu, "Accelerated carbonation curing of foam concrete with lower density", Advanced Materials Research, Vols. 250-253, pp. 172-177, 2011.

[16] B. Zhan, C. Poon, and C. Shi, “CO_2 curing for improving the properties of concrete blocks containing recycled aggregates,” Cement and Concrete Composites, vol. 42, pp. 1–8, 2013.

[17] H. El-Hassan, Y. Shao, and Z. Ghouleh, "Reaction products in carbonation-cured lightweight concrete," Journal of Materials in Civil Engineering, vol. 25, no. 6, pp. 799-809, 2013.

[18] S. Kashef-Haghighi and S. Ghoshal, "CO_2 sequestration in concrete through accelerated carbonation curing in a flow-through reactor," Industrial and Engineering Chemistry Research, vol. 49, no. 3, pp. 1143–1149, 2009.

[19] C. D. Atiş, "Accelerated carbonation and testing of concrete made with fly ash," Construction and Building Materials, vol. 17, no. 3, pp. 147–152, 2003.

[20] L. Mo and D. K. Panesar, "Effects of accelerated carbonation on the microstructure of Portland cement pastes containing reactive MgO," Cement and Concrete Research, vol. 42, no. 6, pp. 769–777, 2012.

[21] V. D. Pizzol, L. M. Mendes, H. Savastano, M. Frías, F. J. Davila, M. A. Cincotto, V. M. John, and G. H. D. Tonoli, "Mineralogical and microstructural changes promoted by accelerated carbonation and ageing cycles of hybrid fiber–cement composites," Construction and Building Materials, vol. 68, pp. 750–756, 2014.

[22] Q. Y. Zou, C. J. Shi, K. R. Zheng, and F. Q. He, "Effect of pre-conditioning on CO_2 curing of block concretes," Journal of Building Materials, vol. 11, no. 1, pp. 116–120, 2008.

[23] D. K. Panesar and L. Mo, "Properties of binary and ternary reactive MgO mortar blends subjected to CO_2 curing," Cement and Concrete Composites, vol. 38, pp. 40–49, 2013.

[24] Y. Shao, "Assessing the carbonation behavior of cementitious materials," Journal of Materials in Civil Engineering, vol. 18, no. 6, pp. 768-776, 2006.

[25] A. Durán-Herrera, J. M. Mendoza-Rangel, E. U. De-Los-Santos, F. Vázquez, P.

Valdez, and D. P. Bentz, "Accelerated and natural carbonation of concretes with internal curing and shrinkage/viscosity modifiers," Materials and Structures, vol. 48, no. 4, pp. 1207–1214, 2014.

[26] ASTM C39 / C39M-15a, Standard test method for compressive strength of cylindrical concrete specimens, ASTM International, West Conshohocken, PA, 2015, www.astm.org.

[27] ASTM C496 / C496M-11, Standard test method for splitting tensile strength of cylindrical concrete specimens, ASTM International, West Conshohocken, PA, 2004, www.astm.org.

[28] C. Rocco, G. V. Guinea, J. Planas, and M. Elices, "Review of the splitting-test standards from a fracture mechanics point of view," Cement and Concrete Research, vol. 31, no. 1, pp. 73–82, 2001.

[29] Zia, Paul, Roberto A. Nunez, Luis A. Mata, and H. M. Dwairi, "Implementation of self-consolidating concrete for prestressed concrete girders," No. FHWA/NC/2006-30. North Carolina Department of Transportation, Research and Analysis Group, 2005.

[30] ASTM C469 / C469M-14, Standard Test Method for Static Modulus of Elasticity and Poisson's Ratio of Concrete in Compression, ASTM International, West Conshohocken, PA, 2014, www.astm.org.

[31] ASTM C1202-12, Standard Test Method for Electrical Indication of Concrete's Ability to Resist Chloride Ion Penetration, ASTM International, West Conshohocken, PA, 2012, www.astm.org.

[32] Neville, Adam M., Properties of Concrete, 3rd edition, Pitman Publishing Inc.,Massachusetts, 1981.

[33] ASTM C157 / C157M-08(2014)e1, Standard Test Method for Length Change of Hardened Hydraulic-Cement Mortar and Concrete, ASTM International, West Conshohocken, PA, 2014, www.astm.org.

[34] Hren, J.J., Goldstein, J., Joy, D.C., Electron microscopy society of America & microbeam analysis society 1979, Introduction to analytical electron microscopy, Plenum Press, New York.

[35] James, Reuben, "X-Ray Diffraction" (2014). A with Honors Projects. Paper 115. http://spark.parkland.edu/ah/115.

[36] Barbara L Dutrow, Louisiana State University and Christine M. Clark, Eastern Michigan University, "X-ray Powder Diffraction (XRD).", Science Research Education Center (SERC). Carleton College, 14 Dec. 2013, http://serc.carleton.edu/research_education/geochemsheets/techniques/XRD.html

[37] The Concrete Society, Permeability testing of site concrete – A review of methods and experience, in Technical Report No. 31. 1987. p. 75.

[38] Ahmad, S., Adekunle, S.K., Maslehuddin, M. & Azad, A.K., "Properties of self-consolidating concrete made utilizing alternative mineral fillers", Construction and Building Materials, vol. 68, pp. 268-276, 2014.

[39] H.-W. Song and S.-J. Kwon, "Permeability characteristics of carbonated concrete considering capillary pore structure," Cement and Concrete Research, vol. 37, no. 6, pp. 909–915, Jun. 2007.

[40] Ramezanianpour, A.A., Pilvar, A., Mahdikhani, M. & Moodi, F., "Practical evaluation of relationship between concrete resistivity, water penetration, rapid chloride penetration and compressive strength", Construction and Building Materials, vol. 25, no. 5, pp. 2472-2479, 2011.

[41] P. Joshi and C. Chan, "Rapid chloride permeability testing," Concrete Construction - World of Concrete, vol. 47, no. 12, pp. 37–43, 2002.

Vitae

Name	Rida Alwi Assaggaf.
Nationality	Yemeni.
Date of Birth	12/06/1987.
Email	ridaalwi@gmail.com
Address	Al-Garn neighborhood, Seiyoun, Hadhramout state.
Academic Background	(2012) Bachelor of science in civil engineering from Hadhramout University of Science and Technology in Mukalla, Yemen. (2016) Master of science in civil engineering (structure) from King Fahd University of Petroleum And Minerals in Dhahran, Saudi Arabia.